Published in final edited form as:

FASEB J. 2020 January ; 34(1): 1247–1269. doi:10.1096/fj.201902163R.

Roles of glycogen synthase kinase 3 alpha and calcineurin in regulating the ability of sperm to fertilize eggs

Souvik Dey[1,*], **Alaa Eisa**[2], **Douglas Kline**[1], **Florence F. Wagner**[3], **Sanjaya Abeysirigunawardena**[4], **Srinivasan Vijayaraghavan**[1]

[1]Department of Biological Sciences, Kent State University, Kent, Ohio, USA.

[2]School of Biomedical Sciences, Kent State University, Kent, Ohio, USA.

[3]Center for the Development of Therapeutics and Stanley Center for Psychiatric Research, The Broad Institute of MIT and Harvard, Cambridge, MA, USA.

[4]Department of Chemistry & Biochemistry, Kent State University, Kent, Ohio, USA.

Abstract

Glycogen synthase kinase 3 (GSK3) was identified as an enzyme regulating sperm protein phosphatase. The GSK3α paralog, but not GSK3β, is essential for sperm function. Sperm lacking GSK3α display altered motility and are unable to undergo hyperactivation, which is essential for fertilization. Male mice lacking sperm specific calcineurin (PP2B), a calcium regulated phosphatase, in testis and sperm, are also infertile. Loss of PP2B results in impaired epididymal sperm maturation and motility. The phenotypes of GSK3α and PP2B knockout mice are similar, prompting us to examine the interrelationship between these two enzymes in sperm. High calcium levels must exist to permit catalytically active calcineurin to function during epididymal sperm maturation. Total and free calcium levels are high in immotile compared to motile epididymal sperm. Inhibition of calcineurin by FK506 results in an increase in the net phosphorylation and a consequent decrease in catalytic activity of sperm GSK3. The inhibitor FK506 and an isoform-selective inhibitor of GSK3α, BRD0705, also inhibited fertilization of eggs *in vitro*. Interrelated functions of GSK3α and sperm PP2B are essential during epididymal sperm maturation and during fertilization. Our results should enable the development of male contraceptives targeting one or both enzymes.

Keywords

GSK3α; fertilization; infertile; calcineurin; male contraceptives

[*]**Corresponding author:** Dr. Souvik Dey, Kent State University, Cunningham Hall (Annex) Rm # A301, PO Box 5190, Kent, OH 44242-0001, Ph: 1-330-672-2941, Fax: (330) 672-3713, sdey4@kent.edu.

Author contributions

S. Dey and S. Vijayaraghavan designed research; S. Dey and A. Eisa performed research; F.F. Wagner contributed new reagents; S. Dey, S. Vijayaraghavan, F.F. Wagner, Abeysirigunawardena and D. Kline analyzed data; S. Dey and S. Vijayaraghavan wrote the paper.

Introduction

In mammals, sperm exiting the seminiferous tubules are immotile and cannot fertilize eggs. There are two key development processes, one occurring in the epididymis and the other in the female reproductive tract. Sperm passing through the epididymis acquire motility and metabolic activation. In the female reproductive tract, motile sperm undergo capacitation and hyperactivation. Hyperactivation is a form of motility essential for sperm passage through the fallopian tube and penetrate the zona pellucida of the egg. Both epididymal initiation of motility and hyperactivation are essential for male fertility.

The capacity for motility already exists in testicular sperm: motility can be induced in demembranated testicular and caput epididymal sperm in the presence of ATP (adenosine triphosphate), cAMP (cyclic-adenosine mono phosphate), appropriate calcium levels and intracellular pH (pH_i). These three second messengers - cAMP, Ca^{2+} and pH_i - also regulate flagellar and ciliary motility in general. Considerable progress has been made in understanding of how sperm cAMP and calcium levels and pH_i change (1, 2). It is known that cAMP acts through a protein kinase (PKA). Loss of cAMP or PKA results in submotile sperm and male infertility (3, 4). The cyclic nucleotide is the product of a unique forskolin insensitive soluble adenylyl cyclase (ADCY10) activated by bicarbonate and calcium (5–7). Increases in cAMP affected by phosphodiesterase inhibitors or bicarbonate, stimulate motility and under some conditions initiate motility in immotile caudal sperm (8–10). Elevation of intracellular pH also leads to similar results (11–13). In the female reproductive tract intra-sperm calcium levels are elevated subsequent to a change in membrane potential and intracellular pH (12, 14). These findings lead to a model wherein cAMP action through PKA is the central tenet of the mechanistic scheme. These models however fall short because they do not incorporate protein phosphatases, which are known to be initiators, modifiers and terminators of signaling responses in cells (15).

We showed that a serine/threonine phosphatase (PP1) has a key role in sperm maturation and regulation of motility (16, 17). The protein phosphatase isoform PP1γ2, present only in mammals, is regulated by its binding proteins – PPP1R2, PPP1R7 and PPP1R11 (18). One or more of these proteins are regulated by kinases glycogen synthase kinase 3 (GSK3). GSK3, PKA and PP1γ2 appear mechanistically interrelated in regulating sperm motility (19). The two isoforms of GSK3α and β, are ubiquitous and redundant in most contexts. We found that one phenotype from the loss of GSK3α in male is infertility (20, 21). Thus, GSK3α is essential in testis and sperm (20). Interestingly the activity of GSK3 declines during epididymal sperm maturation: that is, catalytically active is required in maturing epididymal sperm. Metabolism and ATP generation are also impaired in sperm lacking GSK3α. Sperm lacking GSK3α have altered motility with a stiff mid-piece (21). Inhibition of GSK3 by its non-isoform specific inhibitor, SB216763 resulted in significant decrease in the success rate in IVF assays (19).

Calcineurin (also known as PP2B or PPP3) is a serine/threonine phosphatase regulated by calcium. Calcineurin catalytic (PPP3CC) and regulatory (PPP3R2) subunits are present as testis enriched or testis-specific isoforms (22). Knockout of either *Ppp3CC* or *Ppp3R2* results in male infertility (23). Sperm motility is impaired with a stiffened mid-piece. The

mice are infertile *in vivo*. Sperm from KO mice also could not fertilize eggs *in vitro*. Surprisingly, wild type sperm treated with the calcineurin inhibitors, FK506 and cyclosporine, did not affect *in vitro* fertilization (23). Thus, infertility was thought to be due to impaired sperm function occurring in the male reproductive tract: the epididymis. However, micromolar doses of FK506 has been earlier shown to block sperm acrosomal exocytosis (24).

Phenotypic features of sperm lacking GSK3α and calcineurin appear similar. Immotile epididymal sperm have high activity levels of GSK3 which decline during epididymal sperm maturation (25). Similarly, calcineurin is required for successful epididymal maturation of the mouse sperm (23). This study was undertaken with the goal of exploring the relationship between calcineurin and GSK3 in sperm with an emphasis on the events of sperm capacitation and fertilization.

Materials and methods

Animal ethics statement

All procedures with wild-type (WT) and transgenic mice used in the current study were executed at the Kent State University animal facility, and were approved by the National Institute of Environmental Health Sciences Animal Care and Use Committee and the Kent State Animal Ethics Committee under the Institutional Animal Care and Use Committees protocol number 424 DK 16–14.

Ppp3r2 and *Gsk3α* knock out mice.

The knockout mice were generated by electroporation of Embryonic Stem (ES) cells of B6SJL mice with the designed targeting vector. The targeting sequence contained LacZ and a neo cassette replacing most of exon1, intron1, and 82 base pairs of exon2 with a 5' end homologous to *Ppp3r2* 5'UTR and a 3'end homologous to *Ppp3r2* exon 2. Following homologous recombination, the targeting vector replaced a single *Ppp3r2* allele. The neo cassette (flanked with LoxP sites) was removed from the first generation of transgenic mice through breeding them with Cre+ mice. Transgenic mice produced had LacZ replacing most of exon 1, intron 1, and 82 bp of exon 2. The mice were generated at KOMP Repository (UC, Davis).

For genotyping, ear punches from mice were resuspended in 50μl of alkali lysis buffer (25 mM NaOH and 2 mM EDTA, pH 12.0 in ddH2O) and denatured at 95°C for 1 hr. Next, 50 μl of neutralizing buffer (40 mM Tris-HCl, pH 5.0 in ddH2O) was added. The samples were centrifuged at 1000x*g* and the supernatant was collected for PCR. The primer pair used for detection of 229 bp *Ppp3r2* WT gene were as follows: forward 5'-ATCTTGGTCCTGGATAAGGATGGCG-3'; reverse 5'-AGAGAAACACTTCCGGGTTAGTCG-3'. For the 389 bp LacZ detection the following sets of primers were used: forward 5'-GTTGCAGTGCACGGCAGATACACTTGCTGA-3'; reverse 5'-GCCACTGGTGTGGGCCATAATTCAATTCGC-3'.

Gsk3α knockout mouse line was obtained from Dr. Christopher Phiel, Department of Integrative Biology, University of Colorado, Denver, Colorado, USA. For the wild type

Gsk3α the following primers were used: forward primer 5'-GGGAGTTCTCCAGTCGTGAG-3' and reverse primer 5'-CTTGGCGTTAAGCTCCTGTC-3'; for the global *Gsk3α* knockout, forward primer was 5'-GCCCAATTCCGATCATATTC-3' and reverse primer was same as wild type one. Further details of the *Gsk3α* knockout mice are published (19).

Preparation of sperm cell extracts

For whole cell lysate, sperm were centrifuged at 700×g for 10 min at 4°C. The sperm pellet was resuspended in 1% SDS at a final concentration of 2×10^8 sperm/ml. The sperm suspension in 1% SDS was boiled in a water-bath for 5 min and centrifuged at 12000 × g for 15 min at room temperature and supernatants were used for Western blot analysis. To obtain soluble protein fractions, sperm pellets were resuspended in RIPA lysis buffer (containing 50 mM Tris-HCl, pH 7.4, 150 mM NaCl, 0.25% deoxycholic acid, 1% NP-40, 1mM EDTA) supplemented with 10 mM benzamidine HCl, 0.1% 2-mercaptoethanol, 1 mM PMSF, 1μM calyculin A and 1 mM activated sodium orthovanadate. The sperm suspension was kept on ice for 30 minutes and centrifuged at 16000×g for 20 minutes at 4°C and supernatants were used in the experiments as indicated.

Western blot analysis

The protein fractions were separated on SDS-PAGE and transferred to PVDF membrane. Nonspecific binding sites were blocked with 5% skimmed milk. The PVDF paper was then incubated with primary antibodies: rabbit polyclonal PPP3R2 antibody (Proteintech; Cat # 14005–1-AP); rabbit polyclonal PPP3CC antibody (Proteintech; Cat # 19653–1-AP); β-actin antibody (GeneTex; Cat# GTX109639); rabbit polyclonal phospho-GSK-3α/β Ser21/9 antibody (Cell Signaling #9331); anti-GSK3 α/β mouse monoclonal antibody (44610, Invitrogen); phospho-GSK-3α/β Tyr279/216 antibody (Epitomics; Cat# 2309–1); PP2A Tyr307 antibody (Epitomics; Cat# 1155–1); rabbit polyclonal Phospho-PP1 (Thr320) antibody (Cell Signaling Cat#2581); anti-PP1γ2 antibody (commercially prepared using a synthetic peptide corresponding to the 22 amino acids at the carboxy terminus of PPP1CC2 as the antigen); Axin 1 antibody (Cell Signaling; Cat# C76H11); FKBP-12 antibody (Invitrogen; Cat# PA1–062A); p-GSK3α (Ser21) antibody (Cell Signaling; Cat# 8452S); GSK3α antibody (Cell Signaling; Cat# D80E6); MCT2 antibody (sc-166925); Basigin antibody (R&D Systems; Cat# AF772); 4G-10 p-Tyr antibody (Millipore; Cat# 05–321); p-Ser/Thr PKA substrate antibody (Cell Signaling; Cat# 9621); CatSper1 antibody (sc-271056); Ccnyl1 antibody (sc-514637); IZUMO1 antibody (Biorbyt, Cat# orb34424); Mief1 antibody (sc-514135). All the primary antibodies were usually used at 1:1000 dilution unless specified otherwise. The blots, after washing, were incubated with an appropriate horseradish peroxidase-conjugated secondary antibody (1:2500 dilution) for 1hr. Immunoreactive bands were visualized using a chemiluminescent substrate (Thermo Scientific Super Signal West Pico ECL). The PVDF membrane was re-probed with either rabbit polyclonal β-tubulin (for whole cell extracts) or mouse monoclonal β-actin (for soluble protein extracts) antibodies to verify equal sample loading.

Immunofluorescence labelling testis sections

Testis from wild type (WT) and *Ppp3r2* knockout mice were collected and fixed in 4% paraformaldehyde in PBS at 4°C for 6 hrs. The fixed testes were transferred to 75% ethanol and dehydrated, permeabilized, and embedded in paraffin using a Shandon Tissue Processor (Thermo Electron Corp. Waltham, MA, USA). Multiple 5 μm-thick sections of the whole testis were attached to poly-L-lysine-coated slides, deparaffinized, and rehydrated using a standard procedure (20). Antigen retrieval was performed using 1X Antigen Retrieval Citra Solution (BioGenex, San Ramon, CA, USA). Sections immersed in Citra solution were microwaved 3 times for 2 minutes, with a cooling period of 1 minute between each heating cycle. Slides were incubated for 1 hour at room temperature in a blocking solution containing 5% normal goat serum (Jackson Immuno-research laboratories, West Grove PA) in PBS. Slides were then incubated with rabbit polyclonal primary antibody for PPP3R2 (Proteintech; Cat # 14005–1-AP) (1:200) overnight at 4°C. Slides were washed three times with 1X PBS and incubated with the goat anti-rabbit secondary antibody (1:250) conjugated with Cy3 (Jackson Immunoresearch laboratories, West Grove PA) for 2 hours at room temperature. The slides were washed five times with PBS. Nuclei were labeled with Hoechst dye (Thermo Scientific Pierce, Oregon, and USA). The slides were mounted with Prolong Diamond Antifade Mountant (Thermo Scientific Pierce, Oregon, USA) mounting media, and examined using a Fluo View 500 Confocal Fluorescence Microscope (Olympus, Melville, NY, USA).

Immuno-cytochemical analysis

Caudal epididymal spermatozoa were isolated in PBS from wild type (WT) and *Ppp3r2* knockout mice and were centrifuged at 700×g for 10 min at 4°C. Spermatozoa were fixed in 4% paraformaldehyde, EM grade (Electron Microscopy Sciences) at 4°C for 20 min, followed by permeabilization with 0.2% Triton-X (5 min). Fixed spermatozoa were attached to poly-L-lysine coated coverslips. The coverslips were washed three times with TTBS to remove excess paraformaldehyde and incubated for 4 hours in a blocking solution containing 5% non-immune serum in TTBS at room temperature. The coverslips were incubated overnight at 4°C with one of the following primary antibodies: PPP3R2 antibody (1:150 dilution; Proteintech; Cat # 14005–1-AP), MCT2 (1:200 dilution; sc-166925), Basigin (1:200 dilution; Invitrogen; Cat # 12-1471-81), DRP1 (1:150; BD Biosciences; Cat# 611738) and p-DRP1 (1:150 dilution; Cell Signaling; Cat# 3455S). Coverslips were subsequently washed three times 5 min each with TTBS, followed by incubation with the appropriate secondary antibody conjugated to Cy3 or Alexa flour488 for 1 hour at room temperature. The coverslips were washed three times, 10 min each with TTBS; cells were then stained with Hoechst. Mounting medium was applied, and the slides were examined by confocal laser scanning microscope (Olympus IX81 attached with FLUOVIEW FV1000).

Measurement of intracellular and total calcium in sperm

Spermatozoa were isolated from caput and caudal epididymis of 9–12 weeks old C57BL/6J mice in TBS, pH 7.4 supplemented with 5 mM glucose and 1 mM $CaCl_2$ (26). Sperm were incubated with Fura 2-AM (final conc. 4 μM) at room temperature for 60 min and then washed three times with calcium-free TBS (centrifuged at 700×g for 10 min) to remove

external Fura 2-AM. Basal intracellular Ca^{2+} levels were measured. $CaCl_2$ (1 mM) was added to the cell suspension and immediately digitonin (0.02%) was added, mixed and kept for 10 min to determine the F_{max} value. EGTA solution (20 mM) was then added, mixed and kept for 5 min to determine the F_{min} value. For each time point, fluorescence emission at 510 nm wavelength was measured upon excitation at 340 and 380 nm wavelengths on a Horiba Scientific PTI QM-400 Fluorescence Spectroscopy System (Canada). Continuous readings were taken from 0 to 60 sec. Data were analyzed with FelixGX, version 2.0 software (Photon Technology International, Birmingham, NJ). $[Ca^{2+}]_i$ was calculated using the standard equation (27):

$$\left[Ca^{2+}\right]i = S_f \times Kd \times (R - R_{min})/(R_{max} - R)$$

Where, S_f is the ratio $F_{Ca^{2+}}$ free state excited at 340nm/ $F_{Ca^{2+}}$ saturated state excited at 380nm;

Kd is 220 nM for Fura 2-AM at room temperature;

R is the F_{340}/F_{380} ratio of sample;

R_{min} isthe F_{340}/F_{380} ratio of the negative control (20 mM EGTA);

R_{max} is the F_{340}/F_{380} ratio of the positive control (0.02% digitonin/1 mM $CaCl_2$).

For total calcium measurements, bovine caput and caudal epididymal sperm were washed three times in PBS and centrifuged at 4°C for 10 minutes at 750×g. Sperm pellets were resuspended in a calculated volume of 7% v/v TCA (trichloroacetic acid) at a concentration of 10^8 sperm cells/μl. Sperm suspensions on ice were sonicated twice at amplitude of 60% for 10 seconds each. Following sonication, the samples were centrifuged at 10,000×g for 15 minutes at 4°C. The supernatants were collected and diluted (1:100) with reverse-osmosis (RO) filtered water. Standards were prepared by dissolving calcium chloride in 0.7% v/v TCA in RO filtered water. Calcium in the samples and standards were measured using Flame Photometry (Optima 8×00 ICP-OES, PerkinElmer, MA, USA) (28). Calcium levels are reported as ng/10^8 sperm cells.

In vitro fertilization

9–12 weeks old female C57BL/6J mice were injected intra-peritoneally with 10 IU of pregnant mare's serum gonadotropin (PMSG) hormone. The PMSG injection usually administrated during the light cycle at 4:00 pm. After 52 hours, the females were injected intra-peritoneally with 10 IU of Human chronic gonadotropin (hCG) hormone. WT male mice (3–6 months old) were sacrificed and caudal spermatozoa was isolated in HTF medium. The cell suspension was divided into different parts to be incubated with 1% ethanol (control) or 1% DMSO (control), cyclosporin A (10 μM), FK506 (Tocris, Cat# 3631; ApexBio, Cat# B2143) (at concentrations indicated in the figures), BRD0705 (20 μM) and BRD3731 (10 μM) in 37°C 5% CO_2 incubator for 1 hour. BRD0705 and BRD3731 were obtained from The Broad Institute of MIT and Harvard, Cambridge, MA. Super-ovulated female mice were sacrificed approximately 14 hours after administering hCG. The mice

were dissected and the uteruses, oviducts and ovaries, were removed and placed on PBS media. The oviducts and ovaries were cleaned from any fat tissue under a stereomicroscope. The cleaned oviducts and ovaries were immersed in sterile mineral oil in a fertilization dish. A dissecting needle was used to tear open the ampulla to release the cumulous oocyte complexes (COCs). COCs were removed from the mineral oil into 250 μl drops of HTF medium. For cumulus-free oocyte preparation, 20 μl of hyaluronidase (10 mg/ml) was added to 400 μl drops of HTF containing the COCs under mineral oil and 5–10 min were allowed for the oocytes to be released from the complex. For, zona pellucida-free preparation, this last step was followed by treatment of the oocytes in acidic Tyrode's solution (containing 0.1% PVA) for 30–45 sec. Finally, 15μl of treated sperm cells was transferred from sperm collection dish into the fertilization dish that has COCs, cumulus-free, or zona-free oocytes. The fertilization dishes were incubated in 5% CO_2 and 37°C for 4 hours. The eggs were then transferred from the fertilization droplet into 3 serial wash drops and incubated overnight in 5% CO_2 and 37°C, after which the two cells stage embryos were counted (29).

Sperm motility measurement using CASA

Caudal sperm were incubated under various conditions were diluted to a concentration of 2×10^7 sperm/ml, and 25 μl of diluted sperm suspension was loaded using a large-bore pipette into a 100-lm Leja chamber slide, prewarmed to 37°C. Sperm motility was analyzed with a computer-assisted sperm motility analyzer equipped with the CEROS sperm analysis system (software version 12.3; Hamilton Thorne Biosciences, Beverly, MA) (30). For each chamber with the sperm sample, three to five random fields were recorded and analyzed using the following settings: 90 frames acquired at 60 frames/sec; minimum contrast of 30; minimum cell size at 4 pixels; default cell size at 13 pixels; static cell intensity of 60; low size gate of 0.17; high size gate of 2.26; low-intensity gate of 0.35; high-intensity gate of 1.84; minimum static elongation gate of 0; maximum static elongation gate of 90; minimum average path velocity (VAP) of 50 μm/sec; minimum path straightness (STR) of 50%; VAP cut off of 10 μm/sec; and straight line velocity cut off of 0 μ/sec. Motility was recorded independently for differentially treated sets of sperm samples. To determine the difference between hyperactivated and non-hyperactivated sperm motility parameters sperm were incubated in a capacitation and non-capacitation medium for 90 min followed by analysis by CASA. Spermatozoa exhibiting >100 μm/s VAP, >150 μm/s VCL (curvilinear velocity) and >10 μm ALH (lateral head displacement) were considered to be hyperactivated.

Flow cytometric analysis of sperm acrosome reaction

Mouse caudal sperm were incubated under non-capacitating and capacitating conditions with or without FK506 (20 nM) as stated before. Sperm populations incubated under capacitating medium with or without FK506, were used for IVF with oocytes collected from super-ovulated mice. Post IVF, spermatozoa were collected (including those from non-capacitating medium) and fixed using 4% para-formaldehyde solution. Thereafter, the cells were washed by centrifugation at 700×g for 10 min and resuspended in a medium containing PBS, pH 7.4 with 1 mg/ml $NaBH_4$ at RT to reduce the autofluorescence. Sperm cell populations were washed again and finally dispersed in PBS containing 13.2 μg/ml of PNA-Alexa fluor488 (without any undissolved fluorophores) in and kept at RT for 25 min for staining of acrosome (31, 32). The cells were washed twice with PBS and finally

fluorescence was measured using BD FACSAria with FSC and SSC voltages being 220 and 350, respectively. The fluorescence data was analyzed using BD FACSDiva version 5.0 and FlowJO version 7.2.

In vitro calcineurin activity assay

Spermatozoa were isolated from mouse caput and caudal epididymis in TBS, pH 7.4. Caudal sperm were incubated in non-capacitating and capacitating medium with/without FK506 (20 nM). Intracellular free calcium ion levels were measured using Fura 2-AM as described above. From a duplicate pool of untreated caput and caudal epididymal sperm cells, cellular lysates were prepared using the Calcineurin Cellular Activity Assay Kit, Enzo Life Sciences (BML-AK816) (33). In brief, sperm lysates were prepared using a buffer containing 50 mM Tris, pH 7.5, 0.1 mM EDTA, 0.1 mM EGTA, 1 mM DTT and 0.2% NP-40 along with protease inhibitor cocktail. Background phosphates were removed from the extracts using a kit-provided desalting column. Calcineurin activity assays were performed using the assay buffer (50 mM Tris, pH 7.5, 100 mM NaCl, 6 mM $MgCl_2$, 0.5 mM DTT, 0.25% NP-40 and 0.5 mM $CaCl_2$) in a 50 µl assay volume using 0.15 mM of kit provided substrate (RII phosphopeptide, sequence Asp-LeuAsp-Val-Pro-Ile-Pro-Gly-Arg-Phe-Asp-Arg-Arg-Val-pSer-Val-Ala-Ala-Glu). 5 mM EGTA was used to prepare buffered solutions containing varying concentrations of Ca_2^+ (as measured by intracellular free calcium estimation assay) to be used as equivalent calcium titers present in caput epididymal sperm, caudal epididymal non-capacitated, capacitated and FK506 sperm populations. The cell extracts, assay buffer (with calmodulin) and substrate peptides were incubated for 30 min at ~30°C with/without okadaic acid/ EGTA solution. Another aliquot was with calcium and 20 nM FK506 was used to determine the efficacy of the inhibitor *in vitro*. The reaction was stopped by addition of BIOMOL® REAGENT and colors developed for 20–30 min and the absorbance was measured at 620 nm in microtiter plates (MULTISCAN GO, Thermo Scientific). Different concentrations of phosphate standards (provided with the kit) were used to prepare a standard cure of activity curve from which the activity units of the samples were calculated. One activity unit is defined as the total nmol of phosphate released during the enzymatic reaction.

GSK3 activity assay

RIPA extracts from control or treated sperm from WT or *Ppp3r2* knockout mice were prepared and used for the GSK3 assay as reported (19). GSK3 activity was measured by the amount of $^{32}PO_4$ transferred from [^{32}P] γ- adenosine triphosphate to phospho-glycogen synthase peptide-2 (GSK3 substrate, Millipore). The initial assay buffer contained 200 mM HEPES, 50 mM $MgCl_2$, 8 µM DTT, 5 mM sodium ß-glycerophosphate, 0.4 mM ATP and 4 µCi of gamma-P^{32} ATP. 5µl of this assay buffer was added with 5 µl each of previously prepared cell extract and GS2 peptide (Millipore):YRRAAVPPSPSLSRHSSPHQ-pS-EDEEE(1 mg/ml). The reaction mixture was incubated at 30°C water-bath for 15 min and the reaction was stopped by cooling on ice for 10 minutes. 12-µL aliquot of the reaction mixture was applied to a phosphocellulose cation exchanger (P81; Whatman Inc, Clifton, NJ) paper cut into 1.5cm × 1.5cm squares and washed with 0.1% (vol/vol) phosphoric acid. After 3 washes (5 minutes each) in phosphoric acid, the squares were placed into scintillation vials with 2 mL of distilled water and counted in a scintillation counter.

Lithium-sensitive kinase activity was considered to be due to GSK3. The GSK3 activity was measured as follows: Activity units/10^7 cells = (lithium-sensitive cpm) × (reaction vol/spot vol) / (sp. activity of P^{32} ATP) × reaction time).

Pull down assay

Extracts of caudal spermatozoa from WT and GSK3α knockout mice were prepared by sonication in a hypotonic buffer (containing 20 mM Tris-HCl, pH 7.2, 1 mM $CaCl_2$, 1 mM $MgCl_2$, supplemented with protease inhibitors and 50 nM calyculin A). Extracts were incubated overnight in a rotating shaker at 4°C with 4 μg each of either recombinant PPP3CC-His tag (US Biological, Cat# 374827). Ni-agarose beads were added to the suspension and the incubation continued for 3 hours at room temperature using. After centrifugation and subsequent washing with PBS/10 mM imidazole, the proteins eluted with 200 mM imidazole in PBS were analyzed by western blot (19).

ATP estimation

Caudal epididymal sperm were isolated in TBS, pH 7.4 as described. Sperm were incubated with or without energy substrates for 1 hour at 37°C. Triplicate 50-μl aliquots were diluted into 450 μl of boiling Tris-EDTA buffer (0.1 M Tris-HCl and 4 mM EDTA; pH 7.75) as described previously (34). The diluted suspensions were boiled for 5 min and then frozen on dry ice. The frozen samples were thawed and centrifuged at 15000 × g for 5 min at 4°C. The supernatant was then diluted (usually1:10) using the Tris-EDTA buffer and 100 μl of diluted sample was then utilized for quantifying ATP using the Bioluminescence Assay Kit CLS II (Roche Applied Science). Luminescence was measured in a Turner Biosystems 20/20 Luminometer. To determine the effect of external substrates on ATP levels, sperm were resuspended in pyruvate- and lactate-free TYH medium and incubated with 10 mM glucose or 25 mM lactate. After 2 hours of incubation triplicates aliquots were diluted 1:10 in boiling Tris-EDTA buffer (0.1 M Tris- HCl and 4 mM EDTA; pH 7.75 and used for ATP measurement as described above.

Phosphoprotein enrichment

Phosphoprotein enrichment was carried out as per the manufacturer's protocol using Pro Q Diamond Phospho- enrichment Kit (Invitrogen, cat no. P33361)(35). Caudal epididymal spermatozoa from WT, *Ppp3r2* knockout, and *Gsk3α* knockout mice were collected in TBS. Sperm were washed three times with TBS by centrifugation for 10 min at 700g. Sperm pellet was resuspended in lysis buffer supplemented with endonuclease, protease inhibitors and sodium orthovanadate. Samples were sonicated thrice at 30% amplitude for 10 seconds. Protein estimation was carried out using modified BCA method (36). Enrichment columns were prepared by adding 200μl of ethanol to wet the column. 1 ml of resin was added to each column. Resin was washed twice with 1 ml of deionized water and in the mean while 1 mg of samples were diluted with wash buffer to get the final concentration of 0.1mg/ml. Columns were equilibrated by passing 1ml of wash buffer twice. Diluted samples were passed through the column and flow through was collected. Columns were washed with 1ml of wash buffer thrice and phosphoproteins were eluted five times successively with 250 μl each of elution buffer. Eluted phosphoproteins and the flow through fractions were

concentrated using 3kDa MW cut off filters and a buffer exchange was performed with 25 mM Tris and 0.25% CHAPS and subjected to western blot analysis.

Statistical Analysis

Results are presented as means ± standard errors for at least three observations under identical condition. The data were statistically analyzed by one-way ANOVA AND two-tailed unpaired t-test using Prism, version 7, Graph Pad software (La Jolla, CA). Please see figure legends for further details.

Results

Ppp3r2 knock out mice.

We verified the phenotype of the mice before use in the experiments described. Figure 1A left panel shows the absence of *Ppp3r2* but presence of *LacZ* insert. Western blot in the right panel shows the absence of both the catalytic and regulatory subunits of calcineurin in sperm from the KO mice; this is because when one subunit of calcineurin is absent the other is also degraded (23). Figure 1B confirms the absence of PPP3R2 in testis of calcineurin KO mouse by immuno-histochemistry. Presence of PPP3R2 in wild type mice can be seen (Figure 1C) in the sperm acrosome and mid-piece

Calcium levels in developing epididymal sperm.

The report on the requirement for calcineurin in epididymal sperm did not address a key question (23): how does calcineurin become active in immature caput epididymal sperm? We propose that calcium levels are high in caput compared to caudal epididymal sperm leading to high calcineurin activity in caput sperm. This suggestion is based on studies in bovine which showed that free and total calcium are remarkably high in caput sperm (37). Similar results are reported for mouse epididymal sperm (38). We wished to confirm these findings. Free calcium levels in bovine sperm were determined using single wavelength monitoring of Fura-2 loaded sperm. Dual wavelength monitoring using the ratio of emission from excitation at two different wavelengths is now the preferred method (38, 39). We used dual wavelength monitoring to measure free calcium levels in mouse caput and caudal epididymal sperm. Figure 2A shows a representative trace of Fura 2 fluorescence. Figure 2B illustrates that the free calcium is nearly three-fold higher in caput compared caudal epididymal sperm ~900 nM compared to 300 nM in caudal sperm. We also made these measurements in bovine epididymal sperm. Data in Figure 2C tracing demonstrates that similar to mouse, bovine caput epididymal sperm also have higher levels than caudal sperm confirming data in the earlier report (37). To verify data published more than two decades ago, we also wanted to determine total calcium levels in bovine caput and caudal epididymal sperm. We used bovine rather than the mouse for these measurements because we can obtain larger number and better preparations of epididymal sperm required for the total calcium content measurements. Figure 2D shows that the total calcium levels were 600 ng in caput compared to 300 ng in caudal epididymal sperm. Values are levels in 10^8 spermatozoa. These total calcium levels are comparable to those reported in the earlier report (37).

Effect of calcineurin inhibitors on *in vitro* fertilization.

The report on the requirement for calcineurin for epididymal sperm maturation did not find any effect of calcineurin inhibitors on wild type sperm during capacitation and fertilization: calcineurin inhibitors FK506 and cyclosporine A treated sperm had no effect on IVF (23). This observation is surprising since, the increase of sperm calcium levels known to occur during capacitation should be expected to activate calcineurin suggesting a role for the phosphatase in events essential for fertilization. We decided to verify the reported observations on IVF with the calcineurin inhibitor (). We first ascertained the presence of the FK506 binding protein, FKBP12, by western blot analysis of mouse sperm and testis extracts (Figure 3A - inset) (40). Contrary to the findings in the earlier report, calcineurin inhibitor FK506 at micromolar levels reduced *in vitro* fertilization rates to near zero (Figure 3A). A similar result was obtained with another calcineurin inhibitor cyclosporin A (10 μM). Incubating mouse oocytes rather than sperm with FK506 did not have any effect on IVF. We first used micromolar levels of FK506 were used because these are the concentrations used in the previous study on sperm and cell line (23) (41). Because IVF rates were virtually zero at micromolar concentrations we determined a dose response effect for FK506. There was a concentration dependent inhibition in IVF rates with a maximum inhibition with concentrations as low as 20 nM FK506 (Figure 3B). Two-cell stage embryos seen in Figure 3C (right panel) are representative of the inhibition of IVF seen with FK506 treated compared to untreated sperm (left panel). After incubation in the IVF medium for 3 to 4 hours morphology of sperm was examined. A significant number of spermatozoa, ~19% in FK506 treated vs 6% in control, were bent at their mid-piece. This bent mid-piece morphology was also seen in sperm from *Ppp3cc* (23) and *Gsk3α* knockout mice (21).

Egg plasma membrane is surrounded by a layer of glycoproteins called the zona pellucida and multiple layers of cumulus cells (Figure 3D). We wanted to determine how absence of zona pellucida or cumulus cell will affect fertilization of calcineurin inhibitor treated sperm. *In vitro* fertilization experiments shown in Figure 3C were conducted with eggs surrounded by zona pellucida and cumulus cells. We also examined whether FK506 treated sperm could fertilize zona-free or cumulus-free oocytes. There was no inhibition of fertilization of zona-free eggs with FK506 treated sperm, but IVF was inhibited with cumulus free, zona-intact eggs, (Figure 3E) suggesting that FK506 was impairing the ability of sperm to penetrate the zona pellucida.

Effect of calcineurin inhibition on sperm hyperactivation.

Data in Figure 3 showed that FK506 treated sperm were able to fuse and fertilize eggs lacking the zona pellucida suggesting that inhibitor treated sperm may be unable to penetrate the zona perhaps due to impaired hyperactivation. We determined whether FK506 inhibited sperm hyperactivation. Sperm motility determination using CASA settings to differentiate between capacitated and non-capacitated movement patterns confirmed that hyperactivation parameters were affected in FK506 treated sperm (Figure 4A, 4B). Motility analysis showed that the percent of motility does not differ between sperm incubated under capacitating and non-capacitating conditions (42). However, numbers of motile sperm with higher average path velocity (VAP) and curvilinear velocity (VCL) increase during capacitation and hyperactivation. These higher cut-off values for VAP and VCL along with ALH (lateral

amplitude of head displacement) enable quantification of hyperactivated sperm. Using these cut-off values, FK506 treatment resulted in lower numbers of sperm with VAP >100 um/s and VCL >150 um/s compared to control sperm (Figure 4A). There was also a significant reduction (25%) in ALH of FK506 treated compared to untreated sperm, indicating reduced hyperactivation. Figure 4B shows tracings of the movement of uncapacitated, capacitated, and F506 treated sperm.

Sperm hyperactivation and acrosome reaction follow normal sperm capacitation. Because hyperactivation was affected we next assessed whether FK506 also impaired the ability of sperm to undergo acrosome reaction. Peanut agglutinin was used to measure sperm capacitation (31). Capacitated sperm having undergone acrosome reaction results in a decrease in both the numbers (from ~93% to ~64%) and mean fluorescence intensity (MFI) (~2084 to ~1026) in PNA positive/PI negative cells (Figure 4C). The PNA fluorescence values of FK506 treated sperm resembled non-capacitated sperm. Impaired hyperactivation could be due to the inability of calcineurin to be activated following calcium influx. We measured calcium levels and calcineurin activity of sperm undergoing capacitation in the presence or absence of FK506. Data in Table 1 show that intra sperm calcium levels were high in sperm suspended in a capacitating medium. In addition, calcineurin activity was also high when measured in the presence of the levels of calcium in capacitating sperm. Calcineurin activity in capacitating sperm could also be inhibited by FK506 [0.78 U in control compared to 0.03 U with FK506]. It should be noted that ccalcium levels and calcineurin activity in capacitating sperm (~897 nM Ca^{2+}, 0.78 U calcineurin activity) were comparable to that in immature caput epididymal sperm (~961 nM Ca^{2+}, 1.08 U calcineurin activity).

Relationship between calcineurin and GSK3.

We have previously shown that GSK3 activity is inversely related to its Ser9/21 phosphorylation in developing epididymal sperm (24). Given the observation that calcineurin activity was also high in caput sperm and the sperm motility phenotype of calcineurin KO sperm resembled sperm lacking GSK3a we wanted to see if changes in phosphorylation and activity of GSK3 could be related to changes in the activity of calcineurin during epididymal sperm maturation. Western blot analysis of sperm extracts from WT and *Ppp3r2* KO mice showed that phosphorylation of GSK3α is substantially higher in both caput and caudal in KO compared to wild type sperm. Serine phosphorylation of GSK3β phosphorylation was comparable (Figure 5A) in wild type and knock out sperm. Tyrosine phosphorylation of GSK3 (Tyr-216/279) was also not altered (Figure 5B). There was also no difference in phosphorylation of either isoform in testis of WT and KO mice. Thus, phosphorylation of GSK3α, but not of GSK3β, was increased only in sperm lacking calcineurin. As expected, higher phosphorylation of GSK3α is also reflected in the lower catalytic activity of GSK3 in sperm extracts from KO compared WT mice (Figure 5C). Phosphorylation of sperm protein phosphatase 1 and 2A (Figure 5D) was not affected indicating that a general lowered protein phosphorylation does not occur in sperm lacking calcineurin. Next we wondered whether calcineurin and GSK3a are bound to a complex. There is evidence that GSK3β and calcineurin are bound in extracts from brain (62). Pull down experiments were performed to determine if calcineurin (PPP3CC) interacts with

GSK3α in sperm. We used pull down rather that IP because PPP3R2 and a portion of GSK3α are not entirely in the soluble fraction of sperm extracts. Recombinant His-tagged calcineurin subunit (PPP3CC) appears to specifically pull down GSK3α, but not the β isoform of GSK3 (Figure 5E).

Next, we investigated whether the relationship between calcineurin and GSK3 could be further demonstrated with pharmacological inhibition of calcineurin. We incubated caput epididymal sperm with FK506 and also calyculin A which is an inhibitor of the protein phosphatase PP1. Comparatively, lower inhibitor concentrations (20 nM of FK506 and 5 nM of Calyculin A) are effective in inhibition of caudal PP2B and PP1/PP2A. However, in caput sperm, all these three phosphatases, PP1, PP2A, and PP2B, are considerably more active than caudal sperm. Therefore, we used a higher concentration of FK506 (100 nM) and found that increased phosphorylation of GSK3α can been clearly seen in caput sperm. When FK506 and Calyculin A were used in combination, there is a further increase in GSK3 phosphorylation. It should be noted that with FK506 alone phosphorylation of GSK3α is seen whereas with Calyculin A by itself or in combination with FK506, increases phosphorylation of both GSK3α and β occurs. This suggests that GSK3α isoform is a preferential target of calcineurinBecause there is increase in calcium and calcineurin activity (Table 1) during we wanted to determine if increased calcineurin activity results in decreased GSK3 phosphorylation. Indeed, GSK3α S21 phosphorylation is reduced (Figure 6B) in sperm during capacitation. Data in Figure 6C shows that this decrease in GSK3α phosphorylation during capacitation is dependent upon the presence of external Ca^{2+} in the suspension medium. Thus, it appears that decreased GSK3 phosphorylation is likely a result of calcineurin activation during capacitation. We also examined whether the decrease in GSK3 phosphorylation could be prevented by inhibition of calcineurin. Increasing concentrations of FK506 increased GSK3α phosphorylation (Figure 6D). As expected decreased GSK3α phosphorylation during capacitation is reflected in the increase in GSK3 catalytic activity and FK506 prevented the increase in GSK3 catalytic activity (Figure 6E).

Effect of isoform selective GSK3 inhibitors on IVF.

We have previously shown that sperm treated with the pan-GSK3 inhibitor SB216763, which inhibits both isoforms of GSK3, had lower rates of fertilization in IVF (19). Data above show that GSK3α, but not GSK3β, appears to be a substrate for calcineurin sperm. We therefore wanted to determine whether an isoform-selective inhibition of GSK3α would affect IVF. The compounds BRD0705 and BRD3731 were recently identified as isoform selective inhibitors of GSK3α and GSK3β, respectively (Figure 7A) (23) BRD0705 has been shown to significantly reduce the stimulatory phosphorylation of Tyr-279 of GSK3α in acute myeloid leukemia (AML) cell lines (43) (41). As per their IC_{50} values, BRD3731 has four times higher selectivity on GSK3β than what BRD0705 has on GSK3α; therefore, higher concentration of BRD0705 was used in the study to normalize their effect. Data in Figures 7B, C show that BRD0705, the GSK3α selective inhibitor significantly inhibited IVF by treated sperm. A marginal inhibition seen with the GSK3β selective inhibitor BRD3731 was not statistically significant.

Role of calcineurin in sperm energy metabolism.

Adequate ATP levels are required for normal sperm motility and fertility (21, 44). We compared the ATP levels in sperm from WT and *Ppp3r2* knockout mice. There was no significant difference in ATP levels in KO and WT sperm suspended in buffers without energy substrates or in buffers containing glucose or lactate (Figure 8A). However, ATP levels were significantly lower in KO sperm with pyruvate as an energy substrate suggesting that pyruvate uptake and utilization could be impaired. The monocarboxylate transporter MCT2 and its binding partner, basigin, are thought to regulate pyruvate and lactate transport in cells as discussed later. The levels of both MCT2 and basigin were lower in sperm from calcineurin KO compared to WT mice as seen in western blot of sperm extracts (Figure 8B, upper panel). Both MCT2 and basigin are localized to the midpiece of caudal epididymal sperm (Figure 8B, lower panel). Immunofluorescence also showed lower levels of MCT2 and basigin in KO compared to WT sperm. As shown below phosphorylation of MCT, basigin and proteins implicated mitochondrial fission marker were reduced in sperm lacking calcineurin (45–47).

Effect of FK506 on protein phosphorylation during sperm capacitation.

Increased tyrosine and serine phosphorylation of proteins accompany sperm capacitation (48, 49). Cyclic AMP mediated protein kinase A activation is known to occur during sperm capacitation (3). We determined tyrosine and PKA-mediated serine phosphorylation in FK506 treated sperm. Data in Figure 9A (left panel) shows that treatment of sperm with FK506 results in lower tyrosine phosphorylation compared to control. Serine/threonine phosphorylation detected by PKA phospho-domain antibodies is also altered in FK506 treated sperm (Figure 9A, right panel).

We determined phospho-proteome by tandem MS of extracts of sperm from KO compared to WT mice. We found several proteins which were differentially phosphorylated in the *Ppp3r2* KO compared to WT sperm (data not shown). We used phosphoprotein enrichment followed by western blot to validate changes in phosphorylation of some of the proteins identified by MS. Sperm CatSper channels required for sperm hyperactivation, are known to be modulated by PKA (50). Phosphorylation of CatSper1 is seen to be lower in *Ppp3r2* KO compared to WT sperm. (Figure 9B-I). Figure 9B-II shows that phosphorylation of Ccnyl1, a protein involved in sperm Wnt (51) was significantly reduced in sperm lacking calcineurin (51). Interesting knockout of *Ccnyl1* also results in a bent midpiece in mouse sperm similar to sperm from calcineurin or *Gsk3α* knockout mice. IZUMO1 is a protein present on the sperm outer membrane that binds to Juno, its cognate receptor on egg membrane to initiate the membrane fusion during fertilization (52). Phosphorylation of IZUMO1 was unchanged in the *Ppp3r2* KO sperm (Figure 9B-III). Phosphorylation of a mitochondrial elongation factor, Mief1 known to be involved in mitochondrial fission (47, 53) was lower in the sperm lacking calcineurin (Figure 9B-IV). Mief1 also contains a consensus sequent for GSK3 phosphorylation (Table 2). Monocarboxylate transporters MCT1 and MCT2 responsible for transport of pyruvate and lactate in cells are present in sperm (54). Basigin is a protein complexed to MCT2 (54, 55). Phosphorylation of MCT2 and basigin were significantly reduced (Figure 9B- V, VI) in *Ppp3r2* KO sperm, but that of MCT1 remained unaltered (Figure 9B-VII). The proteins with significant reduction in phosphorylation, CatSper1,

Ccnyl1, Mief1, MCT2 and basigin also contain consensus sequence for GSK3 phsophorylation (Table 2). Calcineurin mediated protein dephosphorylation of DRP1 is known to regulate its translocation to mitochondria and affect mitochondrial fusion and energy potential (56). The fluorescence image (Figure 9C, upper panel) shows that immuno-reactive phospho-DRP1 is visible in sperm from calcineurin KO but not WT mice. Western blot data also show that DRP1 phosphorylation is significantly increased in calcineurin KO sperm (Figure 9C, lower panel).

The calcineurin regulatory subunit PPP3R2 and GSK3α is conserved in mammals.

Testis and sperm contain specific isoforms of the catalytic and regulatory calcineurin, PPP3CC and PPP3R2. The EST database and published information show that the regulatory subunit PPP3R2 is testis specific in its expression (23). Examination of the genomic sequences of shows that PPP3R2 is present only in mammals. PPP3R2 is absent in non-mammalian vertebrates. The first 52 amino acids of N-terminus of PPP3R2, shown here, are conserved in placental mammals and marsupials (Figure 10A). The GSK3α isoform with its extended glycine rich N-terminus, is present in all vertebrates except birds (57). However, the glycine-rich N-terminus of GSK3α is highly conserved only in mammals (Figure 10B).

A model for the function of calcineurin in sperm.

Based on the data above, the possible role of calcineurin in regulating mammalian sperm function is shown in Figure 11. It illustrates that when sperm calcium levels are high in sperm, as seen during capacitation, calcineurin should be activated by its interaction with Ca^{2+}-calmodulin complex. This complex can be inhibited by calcineurin inhibitor, FK506. Activated calcineurin can dephosphorylate and preferentially stimulate GSK3α to phosphorylate its substrates present in sperm midpiece and/ acrosome. Potential substrates of GSK3α which have been found to be differentially phosphorylated in *Ppp3r2* knockout sperm include Mief1, MCT2, basigin, CatSper1 and Ccnyl1. These proteins contain the S/T(p)-X-X-X-S/T consensus sequence present in substrates known to be phosphorylated by GSK3α (Table 2). The protein DRP1 does not contain GSK3 phosphorylation sites but contains sites for calcineurin binding and dephosphorylation. Overall, the proposed mechanism suggests that calcineurin and GSK3α, can together alter the functions of proteins involved in energy transport, mitochondrial function, and calcium influx that can affect hyperactivation and fertilizing ability of sperm.

Discussion

Epididymal sperm maturation and hyperactivation in the female reproductive tract are essential for fertilization. The two signaling enzymes, GSK3α and PPP3R2, are essential for male fertility: deletion of either corresponding genes result in male infertility (20, 21, 23). The sperm phenotypes of the KO are similar. This study explored the relationship between the two signaling enzymes in sperm.

Even though sperm from *Ppp3r2* KO mice were shown to have impaired epididymal sperm maturation the key question of how calcineurin is normally activated during epididymal

sperm maturation was not addressed (23). A report published more than a decade ago showed that high calcium levels in immature caput sperm declined during maturation suggesting that a concomitant decline in calcineurin activity would have followed (37). Two other reports also document high calcium levels in caput compared to caudal sperm (38, 58). However, we wanted to confirm these data in mouse and bovine epididymal sperm. Ratiometric monitoring of Fura 2 loaded cells showed that in mouse, as in bovine, cytosolic calcium levels were two-fold higher in immature caput compared to mature caudal epididymal sperm (Figure 2 A–C). Total calcium levels determined by flame photometry were also higher in caput sperm (Figure 2D). These data further verified previously published results, that showed that high levels of free and total calcium in immature sperm decline during sperm maturation (37, 38). The reasons for the high level of calcium in caput, and its decline in caudal sperm are still unknown. One possibility could be due to a decline in calcium levels in the epididymal luminal fluid. Indeed, it has been reported that the luminal fluid of caput has three-fold higher calcium concentration than the caudal region of the epididymis (38). Further support for the importance of the changes in calcium in the epididymis comes from the observation that knock out of a calcium channel (TrpV6) in the caudal epithelium, prevents the decline of calcium levels in luminal fluid resulting in impaired epididymal sperm maturation and male infertility (59–61). A key conclusion of our study is that high calcineurin activity in caput sperm followed by a decline in its activity in caudal sperm is a key physiological requirement for epididymal sperm maturation. Absence of calcineurin, as in calcineurin knockout mice, or inhibition of calcineurin prevents epididymal sperm maturation resulting in infertility (23). It should be emphasized that similar to calcineurin, catalytic activity of sperm GSK3 also declines during epididymal sperm maturation (25). Loss of GSK3α also impairs sperm maturation resulting in male infertility (20).

The next part of our study was examination of the relationship between sperm calcineurin and GSK3. Sperm from calcineurin knock out mice have markedly higher levels of GSK3 phosphorylation compared to wild type sperm. This variation is due to a difference in phosphorylation and not due to changes in the level of the protein. It is notable that phosphorylation of GSK3α isoform is selectively altered in sperm from KO mice. This increased GSK3α phosphorylation is seen in caput and caudal epididymal sperm but not testis of the knockout mice. There are no significant changes in tyrosine phosphorylation of GSK3 and PP2A or threonine phosphorylation of PP1 suggesting that GSK3α is selectively affected. These data show that GSK3α phosphorylation is directly or indirectly regulated by calcineurin. The enzyme GSK3α does not contain the SLIM sites found in several calcineurin substrates. However, GSK3β has been shown to be a substrate of calcineurin in somatic cells (62). In sperm, GSK3α and calcineurin could be part of a scaffolding complex enabling phosphorylation or dephosphorylation of their substrates. The scaffolding protein axin, which is known to bind GSK3, could be involved (63, 64). Axin has been implicated to play a role in Wnt-signaling in mouse sperm (51). Determination of the exact mechanism by which sperm calcineurin can dephosphorylate GSK3α would require further studies.

The relationship between calcineurin and GSK3α was further revealed by the experiments with the inhibitor FK506. We first used FK506 in caput epididymal sperm, where calcineurin activity is expected to be high, to determine if pharmacological inhibition would

lead to increased GSK3 phosphorylation. Indeed, there was significant difference in GSK3α phosphorylation in FK506 treated compared to control sperm. The observation that GSK3α phosphorylation is reduced in capacitating sperm along with increased calcineurin activity further supported the possibility that phospho-GSK3α is a substrate of calcineurin in sperm. Indeed, FK506 was able to prevent this presumed calcineurin mediated decrease in GSK3α phosphorylation during capacitation. In human sperm, phosphorylation of GSK3α Ser21 has been shown to be significantly decreased during capacitation (65–67). Overall our data with sperm from calcineurin KO mice and with wild type sperm undergoing epididymal sperm maturation and capacitation show that calcineurin is a phosphatase involved in dephosphorylation of GSK3. The interrelationship between GSK3 and calcineurin is a key part of mechanisms underlying sperm maturation in the epididymis and sperm capacitation and hyperactivation during fertilization.

The requirement for calcineurin and GSK3α during fertilization was further examined by pharmacological inhibition of the enzymes during IVF. We found that FK506 was potent in inhibiting IVF – treatment of sperm with 20 nM FK506 reduced IVF rates to near zero. These data are in variance with the report that concentrations of FK506 as high 20 μM had no effect on IVF (23). We emphasize that we used essentially identical conditions as in the previous report for the IVF experiments in our study. The reasons why the previous study found that FK506 had no effect on mouse IVF are not known. Because the GSK3 is a down-stream target of calcineurin, we expected that inhibition of GSK3α should also inhibit IVF. We have previously shown that the inhibitor SB216763 which inhibits both GSK3 isoforms inhibited IVF rates (19). In this study, we used selective inhibitors for either of the two GSK3 isoforms. Figure 7B, 7C shows that GSK3α-selective inhibitor BRD705 inhibited IVF rates of treated sperm. The GSK3β selective inhibitor had little effect on IVF. It should also be noted that the lack of GSK3α or GSK3β in mouse oocytes has no effect on fertilization (68). Thus, the IVF data further reinforce the conclusion that GSK3α and calcineurin are interrelated in the mechanisms underlying sperm maturation in the male reproductive tract and in the female reproductive prior to fertilization of the egg.

Inhibition of calcineurin by FK506 markedly changed the phosphorylation profiles of multiple proteins in sperm (figure 9A–C). The biochemical changes brought about by this calcineurin inhibitor ultimately affected sperm capacitation and hyperactivation process. There is a dramatic increase in the mitochondrial utilization of pyruvate during capacitation (69). Altered mitochondrial energetics including marked changes in phosphorylation of DRP1 and MCT2/basigin in the *Ppp3r2* knockout mice implicates the role of calcineurin in energy metabolism during sperm capacitation and hyperactivation. FK506 treated mouse spermatozoa are unable to fertilize both cumulus-intact and cumulus-free eggs, however fertilization of zona-free eggs was unaffected (figure 3E). These data support the conclusion that FK506 treated sperm are unable to penetrate the zona pellucida of the egg during fertilization.

Intriguingly, both GSK3α and calcineurin are present and conserved only in mammals. PPP3R2 is absent in non-mammalian vertebrates. The glycine-rich N-terminus of GSK3α is highly conserved only in mammals (Figure 10B). This conserved glycine-rich N-terminal is likely to mediate isoform specific localization of GSK3α within sperm. We are actively

examining the role of CENPV (70), a protein enriched in testis (71) and present in sperm, as a potential isoform specific binding protein of GSK3α. The calcineurin along with its regulatory subunit PPP3R2 has been shown to be localized along the sperm flagellum (72), however the binding protein responsible for this localization is not known. The conservation and presence of GSK3α and calcineurin only in mammalian sperm strongly suggest an interrelationship between them in regulating sperm function.

In sum, the signaling enzymes GSK3α being a substrate of calcineurin have key roles both during epididymal sperm maturation in the male reproductive tract and during fertilization in the female reproductive tract. Calcineurin may still have independent essential role in regulating the ability of sperm to fertilize eggs. These findings should lead to a better biochemical understanding of the basis for male infertility and lead to novel approaches to contraception targeting the epididymis and/or sperm in the female reproductive tract.

Acknowledgements

This work was funded by the National Institute of Health (SV): R03HD096176, R21HD086839.

Abbreviations:

GSK3	Glycogen synthase kinase 3
PP2B	Protein phosphatase 2, type B, also referred as calcineurin
ATP	Adenosine triphosphate
cAMP	Cyclic adenosine monophosphate
pHi	Intracellular pH
PKA	Protein kinase A
PP1	Protein phosphatase 1
PP1γ2	PP1 gamma isoform, type 2
PPP1R2/R7/R11	Phospho-protein phosphatase 1, regulator 2/7/11
IVF	In vitro fertilization
Ppp3R2	Phospho-protein phosphatase 3, regulatory subunit type 2
Ppp3CC	Phospho-protein phosphatase 3, catalytic subunit
WT	Wild type
ES cell	Embryonic stem cell
AML	Acute myeloid leukemia
CA	Calyculin A

References

1. Dacheux JL, and Dacheux F (2014) New insights into epididymal function in relation to sperm maturation. Reproduction 147
2. Freitas MJ, Vijayaraghavan S, and Fardilha M (2017) Signaling mechanisms in mammalian sperm motility. Biol Reprod 96, 2–12 [PubMed: 28395326]
3. Nolan MA, Babcock DF, Wennemuth G, Brown W, Burton KA, and McKnight GS (2004) Sperm-specific protein kinase A catalytic subunit Calpha2 orchestrates cAMP signaling for male fertility. Proc Natl Acad Sci U S A 101, 13483–13488 [PubMed: 15340140]
4. Desseyn J-L, Burton KA, and McKnight GS (2002) Expression of a nonmyristylated variant of the catalytic subunit of protein kinase A during male germ-cell development. Proceedings of the National Academy of Sciences 97, 6433–6438
5. Wuttke MS, Buck J, and Levin LR (2001) Bicarbonate-regulated soluble adenylyl cyclase. Journal of the Pancreas 2, 154–158 [PubMed: 11875252]
6. Jaiswal BS, and Conti M (2003) Calcium regulation of the soluble adenylyl cyclase expressed in mammalian spermatozoa. Proceedings of the National Academy of Sciences 100, 10676–10681
7. Xie F, Garcia MA, Carlson AE, Schuh SM, Babcock DF, Jaiswal BS, Gossen JA, Esposito G, van Duin M, and Conti M (2006) Soluble adenylyl cyclase (sAC) is indispensable for sperm function and fertilization. Developmental biology 296, 353–362 [PubMed: 16842770]
8. Jaiswal BS, and Majumder GC (1996) Cyclic AMP phosphodiesterase: a regulator of forward motility initiation during epididymal sperm maturation. Biochem Cell Biol 74, 669–674 [PubMed: 9018374]
9. Majumder GC, Dey CS, Haldar S, and Barua M (1990) Biochemical parameters of initiation and regulation of sperm motility. Systems Biology in Reproductive Medicine 24, 287–303
10. Brokaw CJ (1987) Regulation of sperm flagellar motility by calcium and cAMP-dependent phosphorylation. In Journal of Cellular Biochemistry Vol. 35 pp. 175–184 [PubMed: 2826504]
11. Carr DW, and Acott TS (2005) Intracellular pH Regulates Bovine Sperm Motility and Protein Phosphorylation1. Biol Reprod 41, 907–920
12. Nishigaki T, José O, González-Cota AL, Romero F, Treviño CL, and Darszon A (2014) Intracellular pH in sperm physiology In Biochemical and biophysical research communications Vol. 450 pp. 1149–1158, Academic Press Inc. [PubMed: 24887564]
13. Vijayaraghavan S, Critchlow LM, and Hoskins DD (1985) Evidence for a role for cellular alkalinization in the cyclic adenosine 3',5'-monophosphate-mediated initiation of motility in bovine caput spermatozoa. Biol Reprod 32, 489–500 [PubMed: 2986738]
14. Navarro B, Kirichok Y, and Clapham DE (2007) KSper, a pH-sensitive K+ current that controls sperm membrane potential. Proceedings of the National Academy of Sciences 104, 7688–7692
15. Barford D, Das AK, and Egloff M-P (2002) THE STRUCTURE AND MECHANISM OF PROTEIN PHOSPHATASES: Insights into Catalysis and Regulation. Annual Review of Biophysics and Biomolecular Structure 27, 133–164
16. Vijayaraghavan S, Stephens DT, Trautman K, Smith GD, Khatra B, da Cruz e Silva EF, and Greengard P (1996) Sperm motility development in the epididymis is associated with decreased glycogen synthase kinase-3 and protein phosphatase 1 activity. Biol Reprod 54, 709–718 [PubMed: 8835395]
17. Fardilha M, Esteves SL, Korrodi-Gregorio L, Pelech S, da Cruz ESOA, and da Cruz ESE (2011) Protein phosphatase 1 complexes modulate sperm motility and present novel targets for male infertility. Molecular human reproduction 17, 466–477 [PubMed: 21257602]
18. Goswami S, Korrodi-Gregório L, Sinha N, Bhutada S, Bhattacharjee R, Kline D, and Vijayaraghavan S (2019) Regulators of the protein phosphatase PP1γ2, PPP1R2, PPP1R7, and PPP1R11 are involved in epididymal sperm maturation. Journal of Cellular Physiology 234, 3105–3118 [PubMed: 30144392]
19. Dey S, Goswami S, Eisa A, Bhattacharjee R, Brothag C, Kline D, and Vijayaraghavan S (2018) Cyclic AMP and glycogen synthase kinase 3 form a regulatory loop in spermatozoa. Journal of Cellular Physiology 233, 7239–7252 [PubMed: 29574946]

20. Bhattacharjee R, Goswami S, Dey S, Gangoda M, Brothag C, Eisa A, Woodgett J, Phiel C, Kline D, and Vijayaraghavan S (2018) Isoform-specific requirement for GSK3α in sperm for male fertility. Biol Reprod 99, 384–394 [PubMed: 29385396]
21. Bhattacharjee R, Goswami S, Dudiki T, Popkie AP, Phiel CJ, Kline D, and Vijayaraghavan S (2015) Targeted disruption of glycogen synthase kinase 3A (GSK3A) in mice affects sperm motility resulting in male infertility. Biol Reprod 92, 65 [PubMed: 25568307]
22. Muramatsu T, Giri PR, Higuchi S, and Kincaid RL (2006) Molecular cloning of a calmodulin-dependent phosphatase from murine testis: identification of a developmentally expressed nonneural isoenzyme. Proceedings of the National Academy of Sciences 89, 529–533
23. Miyata H, Satouh Y, Mashiko D, Muto M, Nozawa K, Shiba K, Fujihara Y, Isotani A, Inaba K, and Ikawa M (2015) Sperm calcineurin inhibition prevents mouse fertility with implications for male contraceptive. Science 350, 442–445 [PubMed: 26429887]
24. Bennett JC, Roggero CM, Mancifesta FE, and Mayorga LS (2010) Calcineurin-mediated dephosphorylation of synaptotagmin VI is necessary for acrosomal exocytosis. Journal of Biological Chemistry 285, 26269–26278 [PubMed: 20551332]
25. Somanath PR, Jack SL, and Vijayaraghavan S (2004) Changes in sperm glycogen synthase kinase-3 serine phosphorylation and activity accompany motility initiation and stimulation. J Androl 25, 605–617 [PubMed: 15223849]
26. Dey S, Goswami S, Eisa A, Bhattacharjee R, Brothag C, Kline D, and Vijayaraghavan S (2018) Cyclic AMP and glycogen synthase kinase 3 form a regulatory loop in spermatozoa. J Cell Physiol 233, 7239–7252 [PubMed: 29574946]
27. Grynkiewicz G, Poenie M, and Tsien RY (1985) A new generation of Ca2+ indicators with greatly improved fluorescence properties. In Journal of Biological Chemistry Vol. 260 pp. 3440–3450
28. Hinsvark ON, Wittwer SH, and Sell HM (1953) Flame Photometric Determination of Calcium, Strontium, and Barium in a Mixture. Analytical Chemistry 25, 320–322
29. Nagy A, Gertsenstein M, Vintersten K, and Behringer R (2003) Manipulating the Mouse Embryo Cold Spring Harbor, NY: Cold Spring Harbor Laboratory Press, 814
30. Sinha N, Pilder S, and Vijayaraghavan S (2012) Significant expression levels of transgenic PPP1CC2 in testis and sperm are required to overcome the male infertility phenotype of Ppp1cc null mice. PLoS One 7, e47623 [PubMed: 23082183]
31. Lybaert P, Danguy A, Leleux F, Meuris S, and Lebrun P (2009) Improved methodology for the detection and quantification of the acrosome reaction in mouse spermatozoa. Histology and Histopathology 24, 999–1007 [PubMed: 19554507]
32. Dey S, Roy D, Majumder GC, and Bhattacharyya D (2014) Extracellular regulation of sperm transmembrane adenylyl cyclase by a forward motility stimulating protein. PLoS One 9
33. Garzón-Niño J, Rodríguez-Muñoz M, Cortés-Montero E, and Sánchez-Blázquez P (2017) Increased PKC activity and altered GSK3β/NMDAR function drive behavior cycling in HINT1-deficient mice: Bipolarity or opposing forces. Scientific Reports 7
34. Goodson SG, Qiu Y, Sutton KA, Xie G, Jia W, and O'Brien DA (2012) Metabolic substrates exhibit differential effects on functional parameters of mouse sperm capacitation. Biol Reprod 87, 75 [PubMed: 22837480]
35. Wessel D, and Flügge UI (1984) A method for the quantitative recovery of protein in dilute solution in the presence of detergents and lipids. Analytical Biochemistry 138, 141–143 [PubMed: 6731838]
36. Smith PK, Krohn RI, Hermanson GT, Mallia AK, Gartner FH, Provenzano MD, Fujimoto EK, Goeke NM, Olson BJ, and Klenk DC (1985) Measurement of protein using bicinchoninic acid. Analytical Biochemistry 150, 76–85 [PubMed: 3843705]
37. Vijayaraghavan S, and Hoskins DD (1990) Changes in the mitochondrial calcium influx and efflux properties are responsible for the decline in sperm calcium during epididymal maturation. Molecular reproduction and development 25, 186–194 [PubMed: 2155628]
38. Ecroyd H, Asquith KL, Jones RC, and Aitken RJ (2004) The development of signal transduction pathways during epididymal maturation is calcium dependent. Developmental biology 268, 53–63 [PubMed: 15031104]

39. Dey S, Roy D, Majumder GC, Mukherjee B, and Bhattacharyya D (2015) Role of forward-motility-stimulating factor as an extracellular activator of soluble adenylyl cyclase. Molecular reproduction and development 82, 1001–1014 [PubMed: 26390310]
40. Thomson AW, Bonham CA, and Zeevi A (1995) Mode of action of tacrolimus (FK506): molecular and cellular mechanisms. Ther Drug Monit 17, 584–591 [PubMed: 8588225]
41. Manojlovic Z, Blackmon J, and Stefanovic B (2013) Tacrolimus (FK506) prevents early stages of ethanol induced hepatic fibrosis by targeting LARP6 dependent mechanism of collagen synthesis. PLoS One 8, e65897 [PubMed: 23755290]
42. Goodson SG, Zhang Z, Tsuruta JK, Wang W, and O'Brien DA (2011) Classification of Mouse Sperm Motility Patterns Using an Automated Multiclass Support Vector Machines Model1. Biol Reprod 84, 1207–1215 [PubMed: 21349820]
43. Wagner FF, Benajiba L, Campbell AJ, Weïwer M, Sacher JR, Gale JP, Ross L, Puissant A, Alexe G, Conway A, Back M, Pikman Y, Galinsky I, Deangelo DJ, Stone RM, Kaya T, Shi X, Robers MB, Machleidt T, Wilkinson J, Hermine O, Kung A, Stein AJ, Lakshminarasimhan D, Hemann MT, Scolnick E, Zhang YL, Pan JQ, Stegmaier K, and Holson EB (2018) Exploiting an asp-glu "switch" in glycogen synthase kinase 3 to design paralog-selective inhibitors for use in acute myeloid leukemia. Science Translational Medicine 10
44. COMHAIRE FH, VERMEULEN L, and SCHOONJANS F (1987) Reassessment of the accuracy of traditional sperm characteristics and adenosine triphosphate (ATP) in estimating the fertilizing potential of human semen in vivo. International Journal of Andrology 10, 653–662 [PubMed: 3692615]
45. Benard G, Bellance N, James D, Parrone P, Fernandez H, Letellier T, and Rossignol R (2007) Mitochondrial bioenergetics and structural network organization. Journal of cell science 120, 838–848 [PubMed: 17298981]
46. Chen H, Chomyn A, and Chan DC (2005) Disruption of fusion results in mitochondrial heterogeneity and dysfunction. Journal of Biological Chemistry 280, 26185–26192 [PubMed: 15899901]
47. Zhao J, Lendahl U, and Nistér M (2013) Regulation of mitochondrial dynamics: Convergences and divergences between yeast and vertebrates. In Cellular and Molecular Life Sciences Vol. 70 pp. 951–976
48. Visconti PE, Moore GD, Bailey JL, Leclerc P, Connors SA, Pan D, Olds-Clarke P, and Kopf GS (1995) Capacitation of mouse spermatozoa. II. Protein tyrosine phosphorylation and capacitation are regulated by a cAMP-dependent pathway. Development 121, 1139–1150 [PubMed: 7538069]
49. Puga Molina LC, Luque GM, Balestrini PA, Marín-Briggiler CI, Romarowski A, and Buffone MG (2018) Molecular Basis of Human Sperm Capacitation. Frontiers in Cell and Developmental Biology 6
50. Orta G, De La Vega-Beltran JL, Martín-Hidalgo XD, Santi CM, Visconti PE, and Darszon XA (2018) CatSper channels are regulated by protein kinase A. Journal of Biological Chemistry 293, 16830–16841 [PubMed: 30213858]
51. Koch S, Acebron SP, Herbst J, Hatiboglu G, and Niehrs C (2015) Post-transcriptional Wnt Signaling Governs Epididymal Sperm Maturation. Cell 163, 1225–1236 [PubMed: 26590424]
52. Bianchi E, Doe B, Goulding D, and Wright GJ (2014) Juno is the egg Izumo receptor and is essential for mammalian fertilization. Nature 508, 483–487 [PubMed: 24739963]
53. Yu R, Liu T, Jin SB, Ning C, Lendahl U, Nistér M, and Zhao J (2017) MIEF1/2 function as adaptors to recruit Drp1 to mitochondria and regulate the association of Drp1 with Mff. Scientific Reports 7
54. Mannowetz N, Wandernoth P, and Wennemuth G (2012) Basigin interacts with both MCT1 and MCT2 in murine spermatozoa. Journal of Cellular Physiology 227, 2154–2162 [PubMed: 21792931]
55. Chen C, Maekawa M, Yamatoya K, Nozaki M, Ito C, Iwanaga T, and Toshimori K (2015) Interaction between basigin and monocarboxylate transporter 2 in the mouse testes and spermatozoa. Asian journal of andrology 18, 600

56. Kanamaru Y, Sekine S, Ichijo H, and Takeda K (2012) The phosphorylation-dependent regulation of mitochondrial proteins in stress responses. J Signal Transduct 2012, 931215 [PubMed: 22848813]
57. Alon LT, Pietrokovski S, Barkan S, Avrahami L, Kaidanovich-Beilin O, Woodgett JR, Barnea A, and Eldar-Finkelman H (2011) Selective loss of glycogen synthase kinase-3alpha in birds reveals distinct roles for GSK-3 isozymes in tau phosphorylation. FEBS Lett 585, 1158–1162 [PubMed: 21419127]
58. Morton BE, Sagadraca R, and Fraser C (1978) Sperm motility within the mammalian epididymis: species variation and correlation with free calcium levels in epididymal plasma. Fertility and sterility 29, 695–698 [PubMed: 658483]
59. Weissgerber P, Kriebs U, Tsvilovskyy V, Olausson J, Kretz O, Stoerger C, Vennekens R, Wissenbach U, Middendorff R, Flockerzi V, and Freichel M (2011) Male fertility depends on Ca2+ absorption by TRPV6 in epididymal epithelia. Science Signaling 4
60. Weissgerber P, Kriebs U, Tsvilovskyy V, Olausson J, Kretz O, Stoerger C, Mannebach S, Wissenbach U, Vennekens R, Middendorff R, Flockerzi V, and Freichel M (2012) Excision of Trpv6 gene leads to severe defects in epididymal Ca2+ absorption and male fertility much like single D541A pore mutation. J Biol Chem 287, 17930–17941 [PubMed: 22427671]
61. Jenkins AD, Lechene CP, and Howards SS (1980) Concentrations of seven elements in the intraluminal fluids of the rat seminiferous tubules, rate testis, and epididymis. Biol Reprod 23, 981–987 [PubMed: 7470534]
62. Kim Y, Lee YI, Seo M, Kim SY, Lee JE, Youn HD, Kim YS, and Juhnn YS (2009) Calcineurin dephosphorylates glycogen synthase kinase-3 beta at serine-9 in neuroblast-derived cells. Journal of Neurochemistry 111, 344–354 [PubMed: 19659461]
63. Jope RS, and Johnson GV (2004) The glamour and gloom of glycogen synthase kinase-3. Trends in biochemical sciences 29, 95–102 [PubMed: 15102436]
64. Fraser E, Young N, Dajani R, Franca-Koh J, Ryves J, Williams RSB, Yeo M, Webster MT, Richardson C, Smalley MJ, Pearl LH, Harwood A, and Dale TC (2002) Identification of the Axin and Frat binding region of glycogen synthase kinase-3. Journal of Biological Chemistry 277, 2176–2185 [PubMed: 11707456]
65. Andò S, and Aquila S (2006) Arguments raised by the recent discovery that insulin and leptin are expressed in and secreted by human ejaculated spermatozoa In Molecular and Cellular Endocrinology Vol. 245 pp. 1–6, Elsevier Ireland Ltd
66. Aquila S, Gentile M, Middea E, Catalano S, Morelli C, Pezzi V, and Andò S (2005) Leptin secretion by human ejaculated spermatozoa. Journal of Clinical Endocrinology and Metabolism 90, 4753–4761 [PubMed: 15944217]
67. Aquila S, Guido C, Middea E, Perrotta I, Bruno R, Pellegrino M, and Andò S (2009) Human male gamete endocrinology: 1alpha, 25-dihydroxyvitamin D3 (1,25(OH)2D3) regulates different aspects of human sperm biology and metabolism. Reproductive Biology and Endocrinology 7
68. Monteiro da Rocha A, Ding J, Slawny N, Wolf AM, and Smith GD (2015) Loss of glycogen synthase kinase 3 isoforms during murine oocyte growth induces offspring cardiac dysfunction. Biol Reprod 92, 127 [PubMed: 25833158]
69. du Plessis S, Agarwal A, Mohanty G, and van der Linde M (2014) Oxidative phosphorylation versus glycolysis: what fuel do spermatozoa use? Asian journal of andrology 17, 230
70. Honda Z, Suzuki T, and Honda H (2009) Identification of CENP-V as a novel microtubule-associating molecule that activates Src family kinases through SH3 domain interaction. Genes Cells 14, 1383–1394 [PubMed: 19930468]
71. Yue F, Cheng Y, Breschi A, Vierstra J, Wu W, Ryba T, Sandstrom R, Ma Z, Davis C, Pope BD, Shen Y, Pervouchine DD, Djebali S, Thurman RE, Kaul R, Rynes E, Kirilusha A, Marinov GK, Williams BA, Trout D, Amrhein H, Fisher-Aylor K, Antoshechkin I, DeSalvo G, See LH, Fastuca M, Drenkow J, Zaleski C, Dobin A, Prieto P, Lagarde J, Bussotti G, Tanzer A, Denas O, Li K, Bender MA, Zhang M, Byron R, Groudine MT, McCleary D, Pham L, Ye Z, Kuan S, Edsall L, Wu YC, Rasmussen MD, Bansal MS, Kellis M, Keller CA, Morrissey CS, Mishra T, Jain D, Dogan N, Harris RS, Cayting P, Kawli T, Boyle AP, Euskirchen G, Kundaje A, Lin S, Lin Y, Jansen C, Malladi VS, Cline MS, Erickson DT, Kirkup VM, Learned K, Sloan CA, Rosenbloom KR, De Sousa BL, Beal K, Pignatelli M, Flicek P, Lian J, Kahveci T, Lee D, Kent WJ, Santos MR, Herrero

J, Notredame C, Johnson A, Vong S, Lee K, Bates D, Neri F, Diegel M, Canfield T, Sabo PJ, Wilken MS, Reh TA, Giste E, Shafer A, Kutyavin T, Haugen E, Dunn D, Reynolds AP, Neph S, Humbert R, Hansen RS, De Bruijn M, Selleri L, Rudensky A, Josefowicz S, Samstein R, Eichler EE, Orkin SH, Levasseur D, Papayannopoulou T, Chang KH, Skoultchi A, Gosh S, Disteche C, Treuting P, Wang Y, Weiss MJ, Blobel GA, Cao X, Zhong S, Wang T, Good PJ, Lowdon RF, Adams LB, Zhou XQ, Pazin MJ, Feingold EA, Wold B, Taylor J, Mortazavi A, Weissman SM, Stamatoyannopoulos JA, Snyder MP, Guigo R, Gingeras TR, Gilbert DM, Hardison RC, Beer MA, and Ren B (2014) A comparative encyclopedia of DNA elements in the mouse genome. Nature 515, 355–364 [PubMed: 25409824]

72. Chung JJ, Shim SH, Everley RA, Gygi SP, Zhuang X, and Clapham DE (2014) Structurally distinct ca(2+) signaling domains of sperm flagella orchestrate tyrosine phosphorylation and motility. Cell 157, 808–822 [PubMed: 24813608]

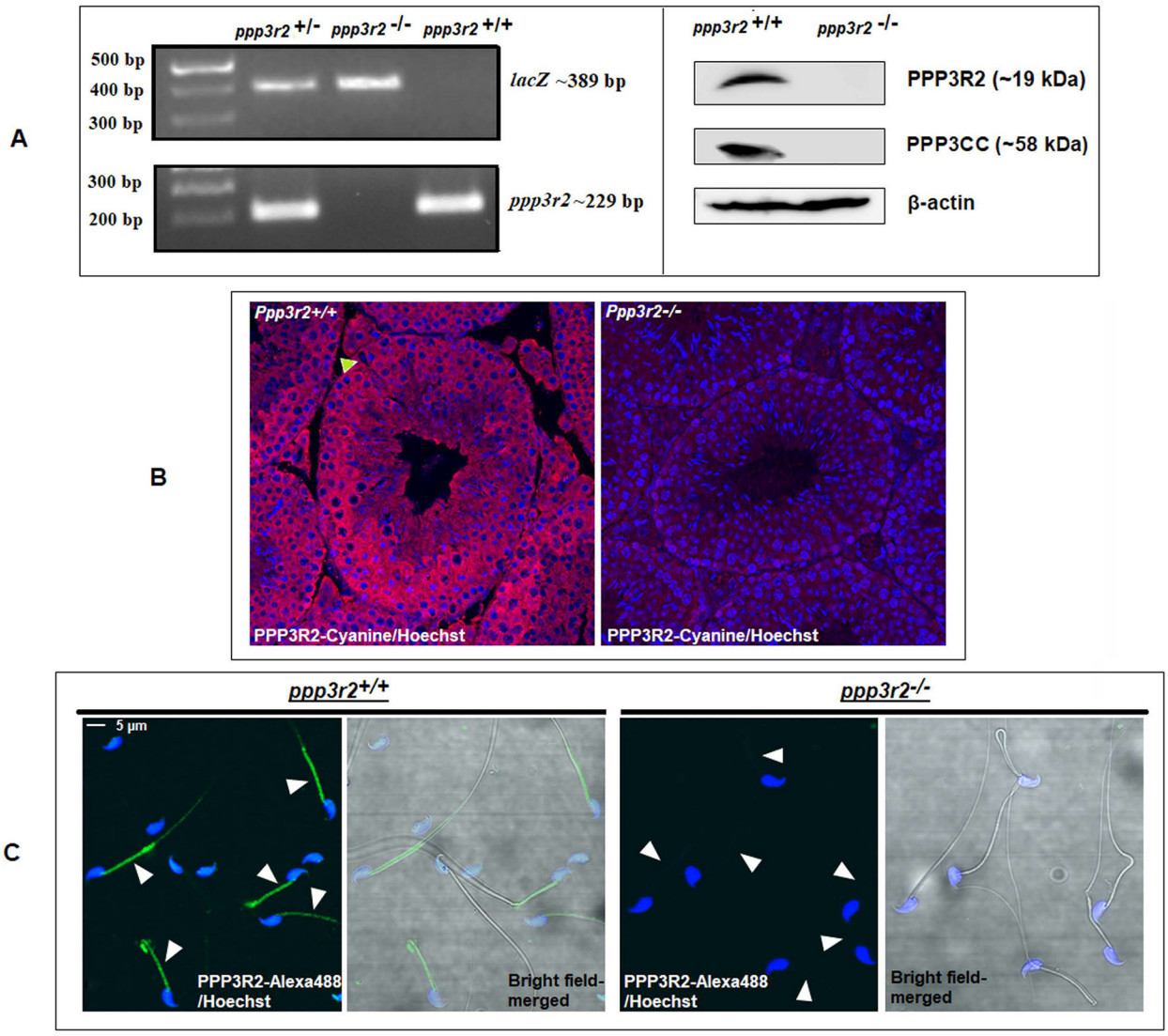

Figure 1. Characterization of the calcineurin regulatory subunit in WT and *Ppp3r2* knockout mice.

A) Genotyping of knockout mice by PCR using primers designed to the detect the presence of knock out allele (containing LacZ reporter gene), as described in the materials and methods section, shows absence of *Ppp3r2*. Figure in the right panel is the western blot analysis of sperm cell extracts from KO and wild type mice using specific antibodies shows the absence of PPP3R2 in KO mice. B) Immunostaining of adult testis sections shows absence of PPP32 in knockout mice while it is present within the seminiferous tubules of the testis of wild type mice; green arrow indicates the absence of PPP3R2 in Sertoli cell. Hoechst dye was used to identify nuclei. C) Sperm permeabilized with 0.5% Triton X-100 and fixed with paraformaldehyde and stained with rabbit PPP3R2 antibodies followed by Alexa fluor-488 labelled secondary antibodies. The merged figures in the left of each panel shows localization of the protein mainly in the midpiece and dimly in the principal piece of sperm from wild type sperm while there is no detectable signal in sperm from knock out mice.

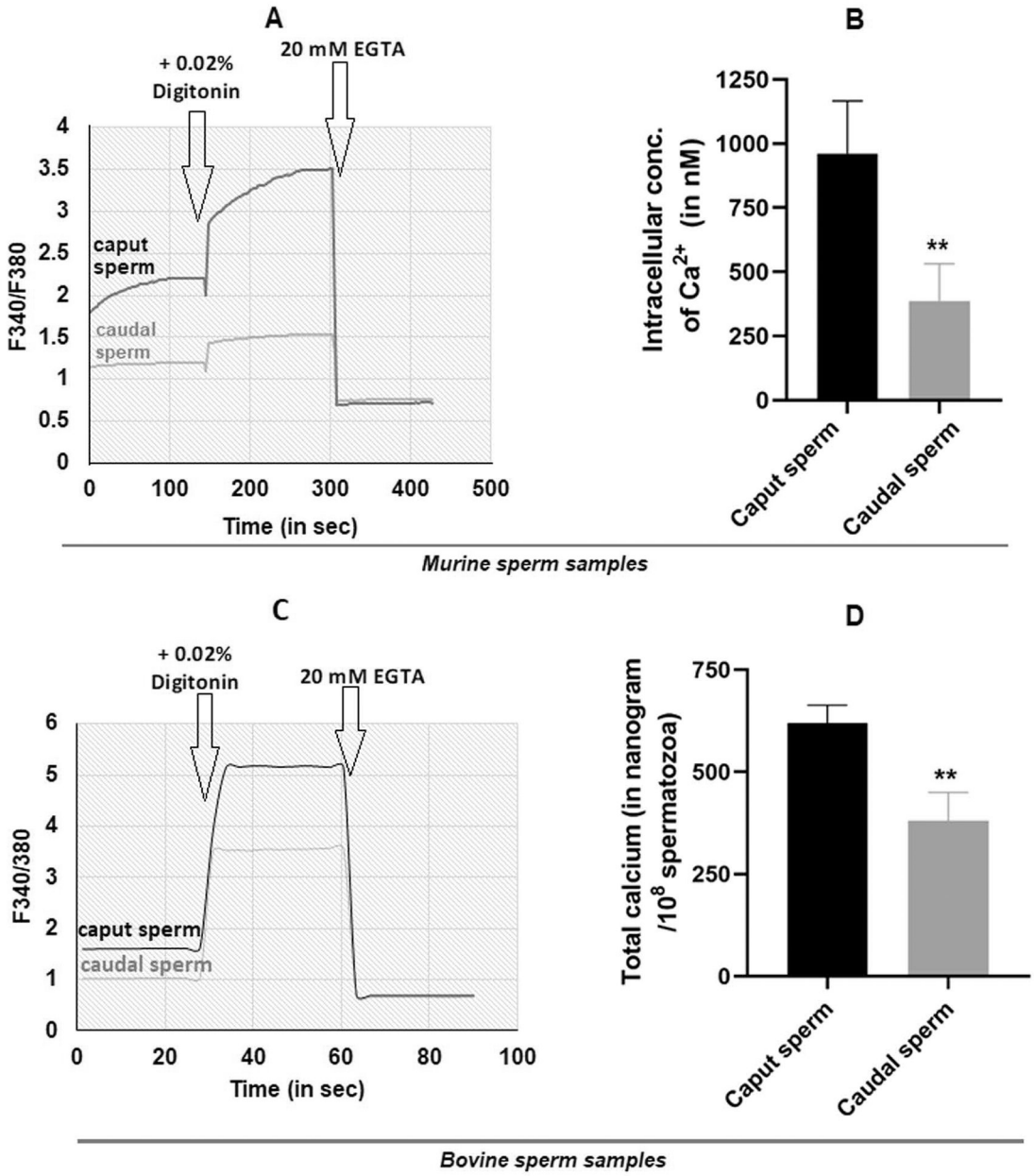

Figure 2: Calcium levels in epididymal spermatozoa.

Representative plots, showing intracellular free Ca^{2+} measured spectro-fluorometrically using Fura 2-AM. Mouse caput and caudal spermatozoa were incubated with 4μM Fura 2AM in a buffer containing 1 mM calcium. Fura 2 loaded sperm were monitored on a dual wavelength spectro-photometer and the calcium tracers obtained as described in materials and methods. Mouse sperm (A) and bovine sperm (C). The bar diagram shows intracellular calcium levels in mouse epididymal sperm measured in 4 different experiments. Values are means ± SEM. (D) Total calcium levels of twice washed bovine caput and caudal spermatozoa were measured by flame photometry as described in the materials and methods Data are means ± SEM (n=5). **p ≤0.01.

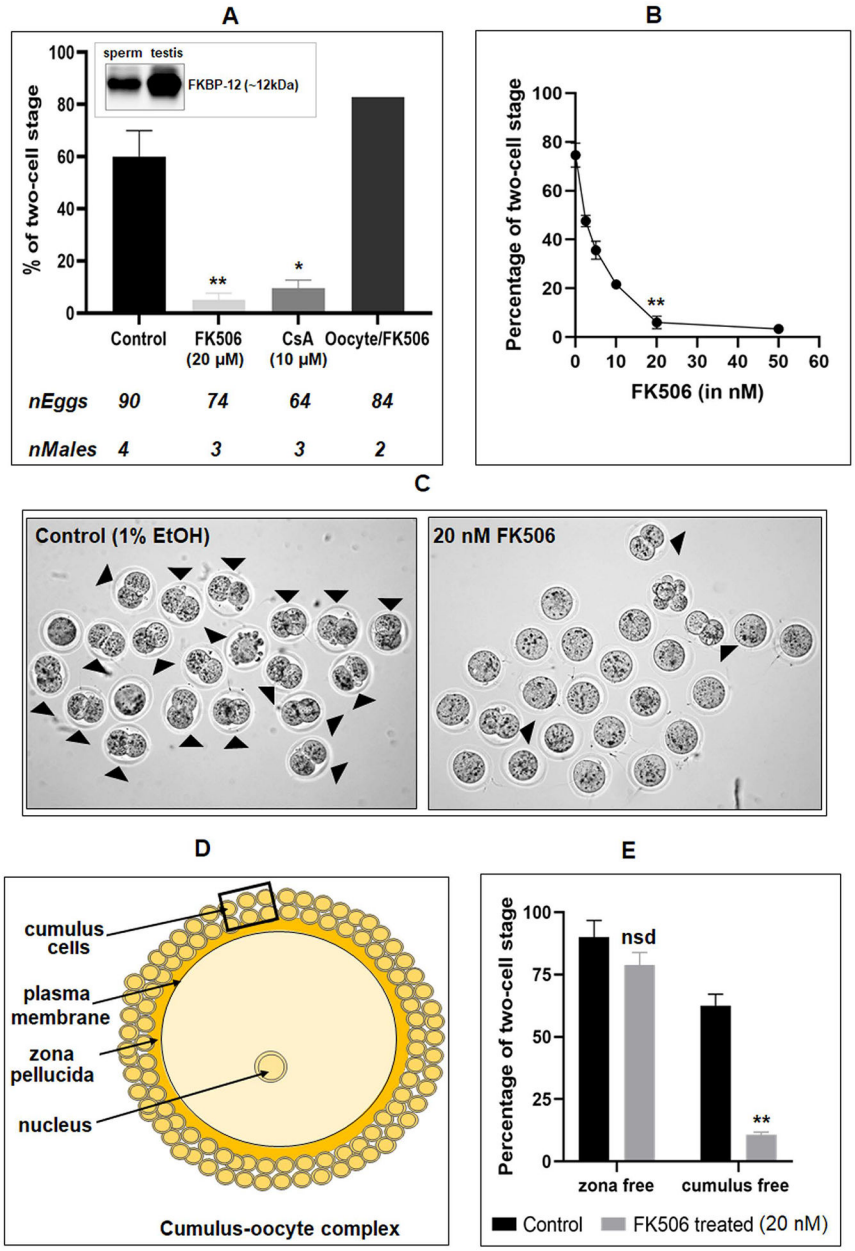

Figure 3. Effect of calcineurin and GSK3 inhibitors on *in vitro* fertilization

A) Western blot shows presence of FK506 binding protein, FKBP12, in mouse sperm and testis lysates (Inset). Spermatozoa were incubated under capacitating conditions with 1% ethanol (control), FK506 (20 μM), or cyclosporin A (10 μM). In the last set, oocytes were treated with FK506 (20 μM) and incubated with untreated spermatozoa. B) Dose response curve of FK506 with 0, 2.5, 5, 10, 20 & 50 nM concentration showing almost complete inhibition of fertilization at 20 nM. Data are mean ± SEM of 3 different experiments. *p ≤0.05 versus control. C) Bright-field images of the two-cell stage embryos resulting from the IVF experiments. Images are representative of the experiments shown in the figure 3B. D) A schematic presentation of cellular composition of a typical cumulus-oocyte complex (COC) showing different levels of barriers that sperm cells need to cross to fertilize an egg. E)

Cumulus cells were removed using 0.05% hyaluronidase, while zona pellucida layer was dissolved by acidic Tyrode's solution. FK506 (20 nM) treated spermatozoa used for IVF of cumulus free zona intact oocytes were unable to fertilize the eggs, while same used for zona-free oocytes showed no difference compared to the control. Data are mean ± SEM of 3 different experiments. *p ≤0.05 versus control.

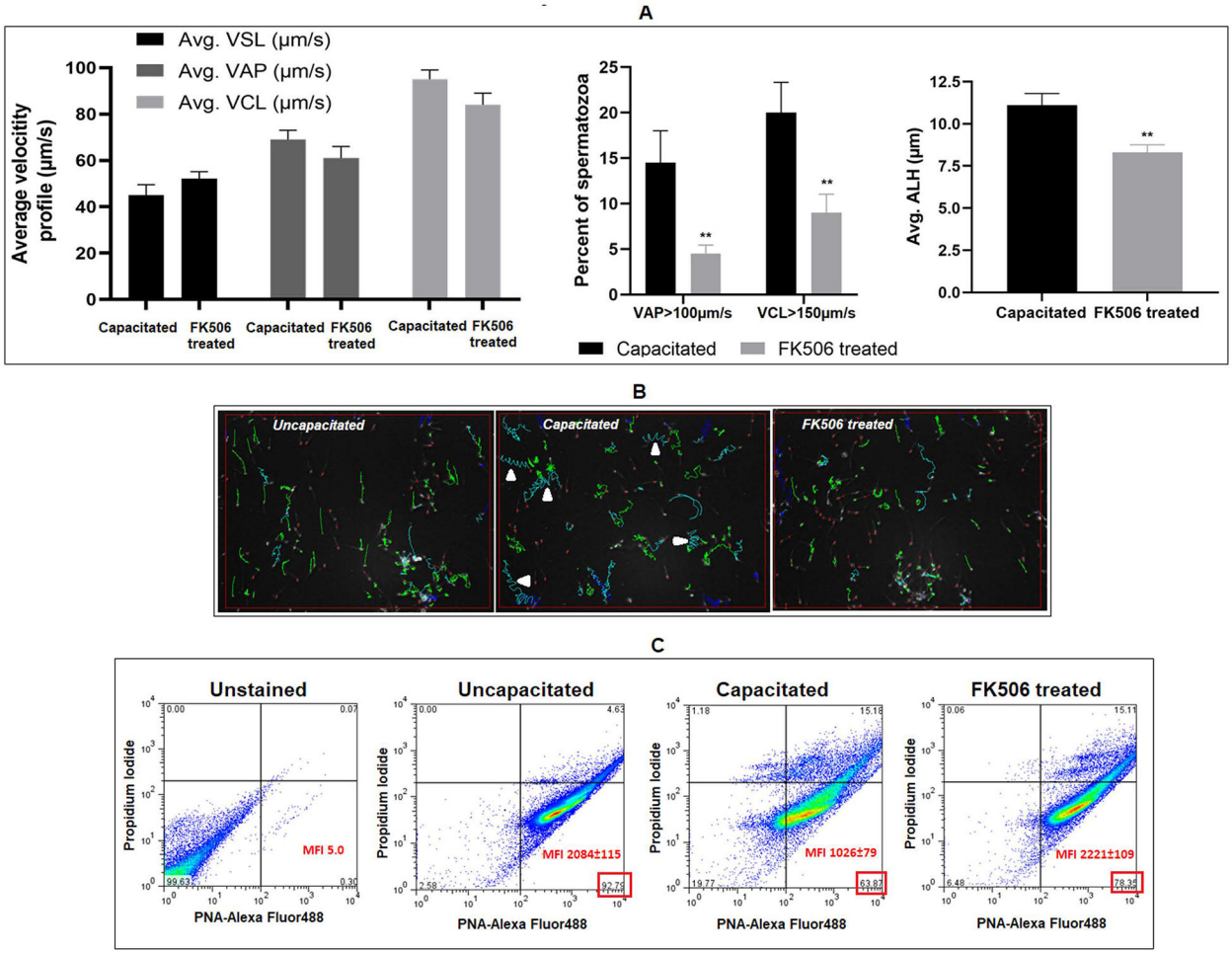

Figure 4: Effect of FK506 hyperactivation of sperm motility and acrosome reaction.

A) Sperm were incubated (3 hrs) under non capacitating conditions or capacitating conditions in the absence or presence of 20 nM FK506 followed by motility analysis by CASA using parameter settings to detect hyperactivation as described in the materials and methods. FK506 prevents increase of sperm average path velocity (VAP), curvilinear velocity (VCL) (beyond certain threshold values as indicated) and lateral head amplitude (ALH), seen in control sperm incubated under capacitating conditions. B) Depiction of sperm movement in capacitated and FK506 treated sperm cells; green tracings denote low-amplitude movements, while blue tracings indicate high-amplitude movements of the sperm; red dots indicate stationary sperm cells; arrow indicates high-lateral head amplitude movements of sperm signifying hyperactivation. C) Sperm cells were analyzed using acrosome specific probe PNA-Alexa fluor 488 and propidium iodide (PI). Sperm populations incubated under capacitating medium with or without FK506, were used for IVF with oocytes collected from super-ovulated mice. Post IVF, spermatozoa were collected and fixed using 4% para-formaldehyde solution, stained with PNA-Alexa fluor 488 and PI and, subsequently used for flow-cytometric analysis. Capacitated sperm population that has undergone acrosome reaction showed decrease in both numbers and mean fluorescence intensity (MFI) in PNA positive/PI negative cells indicating loss of the acrosomes; however,

this was not the case in the FK506 treated sperm which largely resembled the non-capacitated sperm population. Values are from 4 different mice presented as mean±SEM.

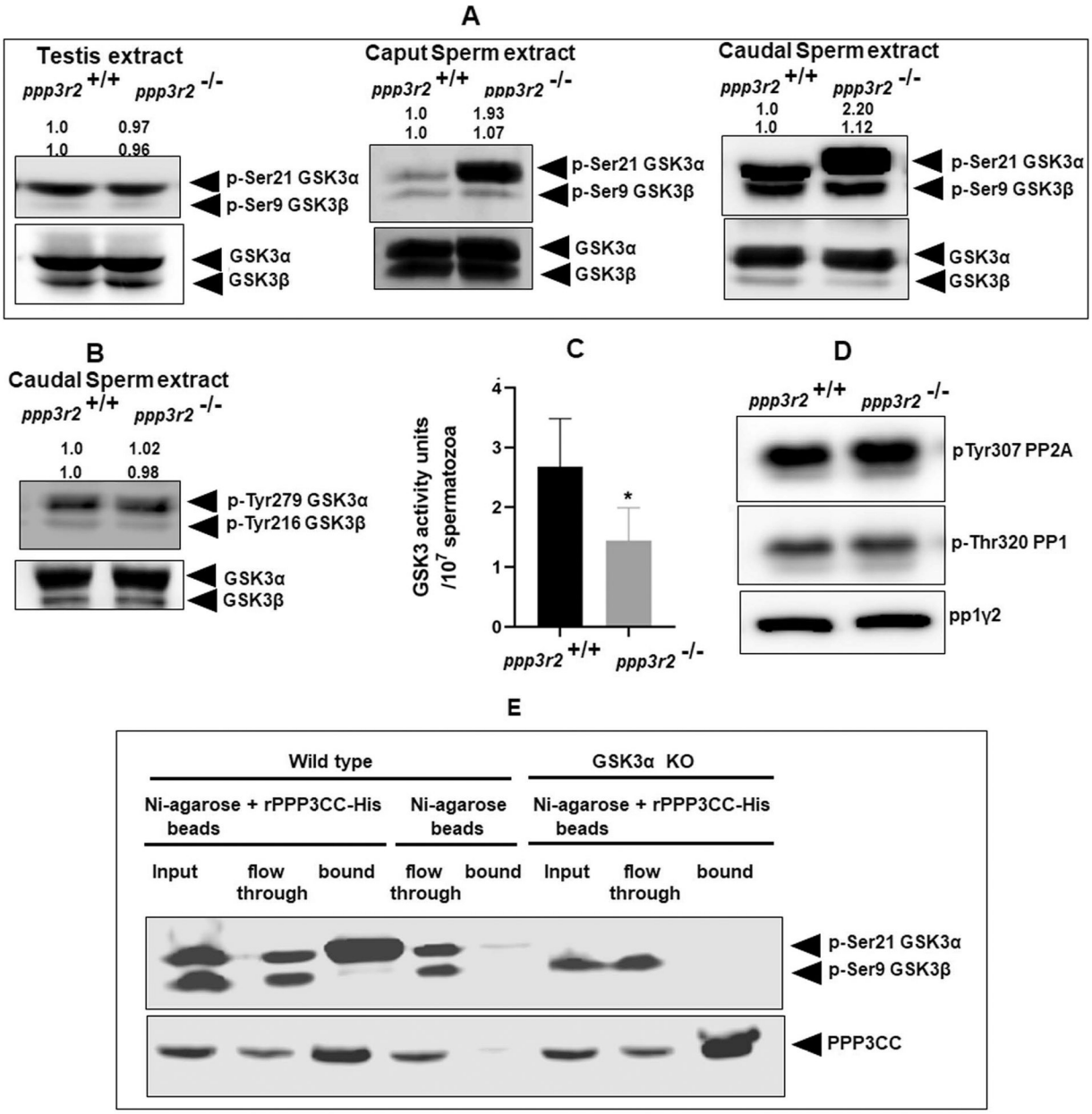

Figure 5. Relationship between sperm GSK3 and calcineurin.

(A) Testis and sperm extract from wild type and knock out mice were subject to western blot analysis developed with antibodies against GSK3α/β-pSer21/pSer9. There was no difference in phosphorylation in testis while there is increased phosphorylation of GSK3α in both caput and caudal sperm from knock out compared to wild type mice as indicated by the calculated average band intensities (n=4) provided on top of the corresponding blots. (B) Representative blot developed with antibodies against pYGSK3 shows no change in tyrosine phosphorylation of GSK3 in KO and wild type sperm as indicated by the average band intensities (n=3) provided on top of the blot. C) Catalytic activity of GSK3 was measured using GS2 peptide as a substrate as described under materials and methods. Unit activity is defined as nmoles of $^{32}PO_4^{2-}$ incorporated/min/10^7 sperm. Catalytic activity of GSK3 is

significantly reduced in KO compared to wild type caudal sperm. Values are means ± SEM (n=4); *p ≤0.05. D) Phosphorylation of PP2A and PP1γ2 in sperm from knockout mice are unchanged compared to wild type sperm. E) Pull-down assay using His tagged recombinant calcineurin catalytic subunit [PPP3CC-His] suggesting that GSK3α and PPP3CC could be part of a complex. Blots were developed with anti-rabbit PPP3CC and anti-mouse GSK3αβ antibodies as described under materials and methods. Flow through denotes unretained protein, while bound signifies pulled-down protein fraction. In the control, only Ni-agarose beads were used, but not recombinant PPP3CC.

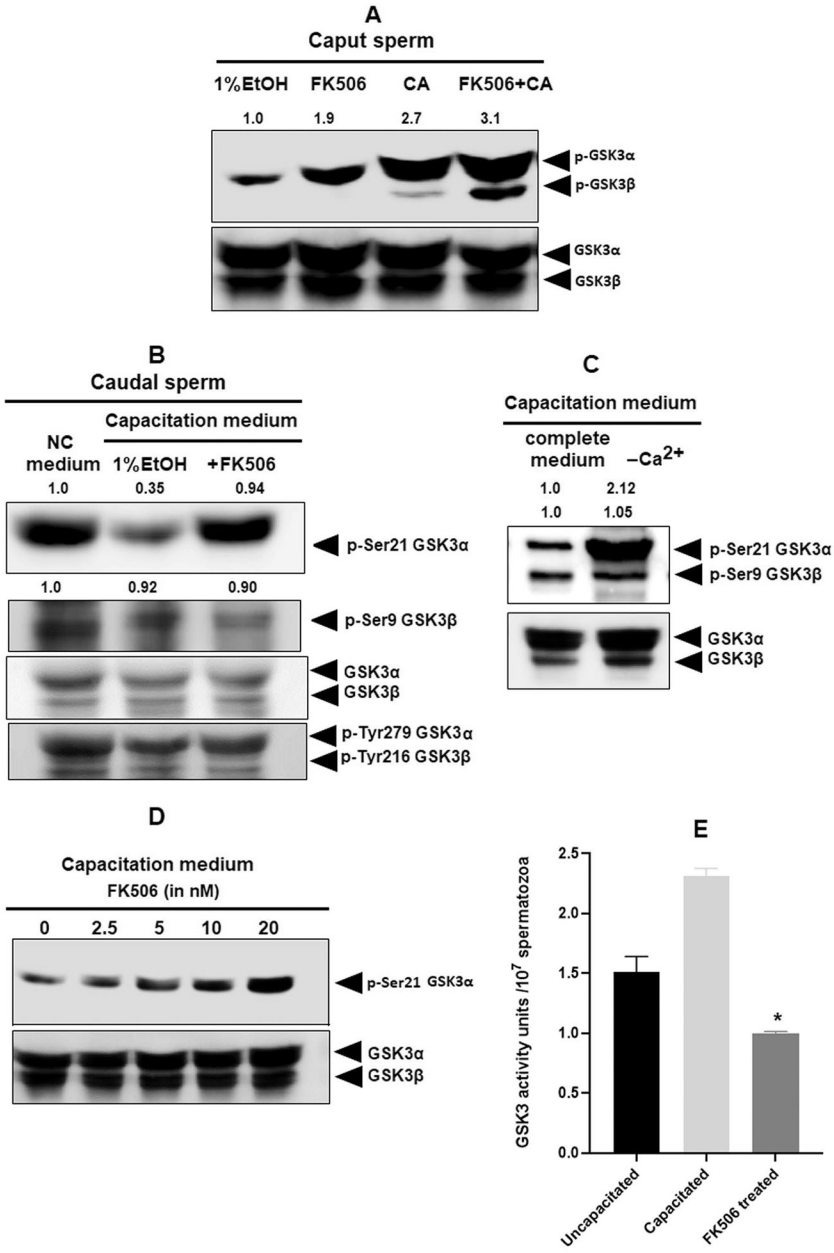

Figure 6. Effect of calcineurin inhibition on GSK3α phosphorylation in epididymal mouse spermatozoa.

A) Caput sperm were incubated with or without FK506 (20 nM) and calyculin A (5nM). Extracts were subject to western blot analysis with GSK3α/β-pSer21/pSer9 antibodies. There was clear increase in GSK3α phosphorylation in sperm treated with FK506, but both GSK3α and β increases with calyculin A; only GSK3α phosphorylation band intensities were quantified. B) Mouse caudal epididymal spermatozoa were incubated for 90 min under capacitating or non-capacitating conditions with or without FK506 (20nM) as described under materials and methods. Western blot analysis of sperm extracts following this incubation were subject to western blot analysis developed with GSK3αβ-pSer9/21 antibodies. Capacitation results in lowered GSK3α phosphorylation which is reversed in the

presence of FK506 as indicated by the calculated average band intensities (n=3) provided on top of the corresponding blots. C) Lowered GSK3α phosphorylation is seen in sperm incubated in a capacitating medium in the presence but not in the absence calcium. Requirement of extracellular calcium for changes in GSK3 phosphorylation and activity. D) Spermatozoa were treated with the indicated concentrations of FK506 for 90 min; western blot developed with GSK3α-pSer21 antibodies show a FK506 dose dependent increase in the phosphorylation. E) GSK3 activity was measured using a GS2 peptide substrate and ^{32}ATP as described for Figure 3C and under materials and methods.

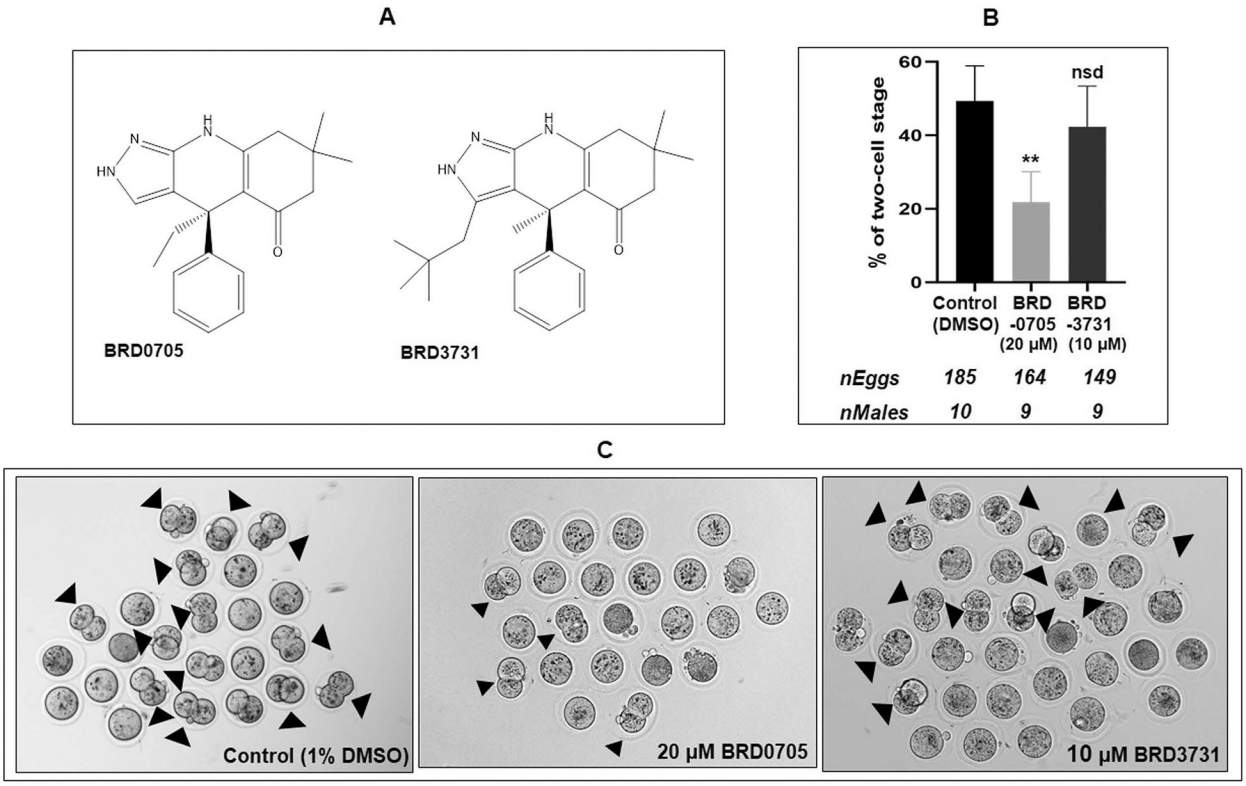

Figure 7: Effect of isoform-selective inhibitors of GSK3α or GSK3β on its in vitro fertilization ability.

A) Chemical structure of GSK3α inhibitor, BRD0705 and GSK3β inhibitor, BRD3731 (43). B) Spermatozoa were incubated with BRD0705 (20μM) and BRD3731 (10μM) under capacitating condition for 90 min and used for IVF; BRD0705 significantly inhibited the fertilization of eggs whereas the GSK3β inhibitor BRD3731 had no effect compared to control. C) Representative bright-field pictures of two-cell embryo formation corresponding to the treatments described above.

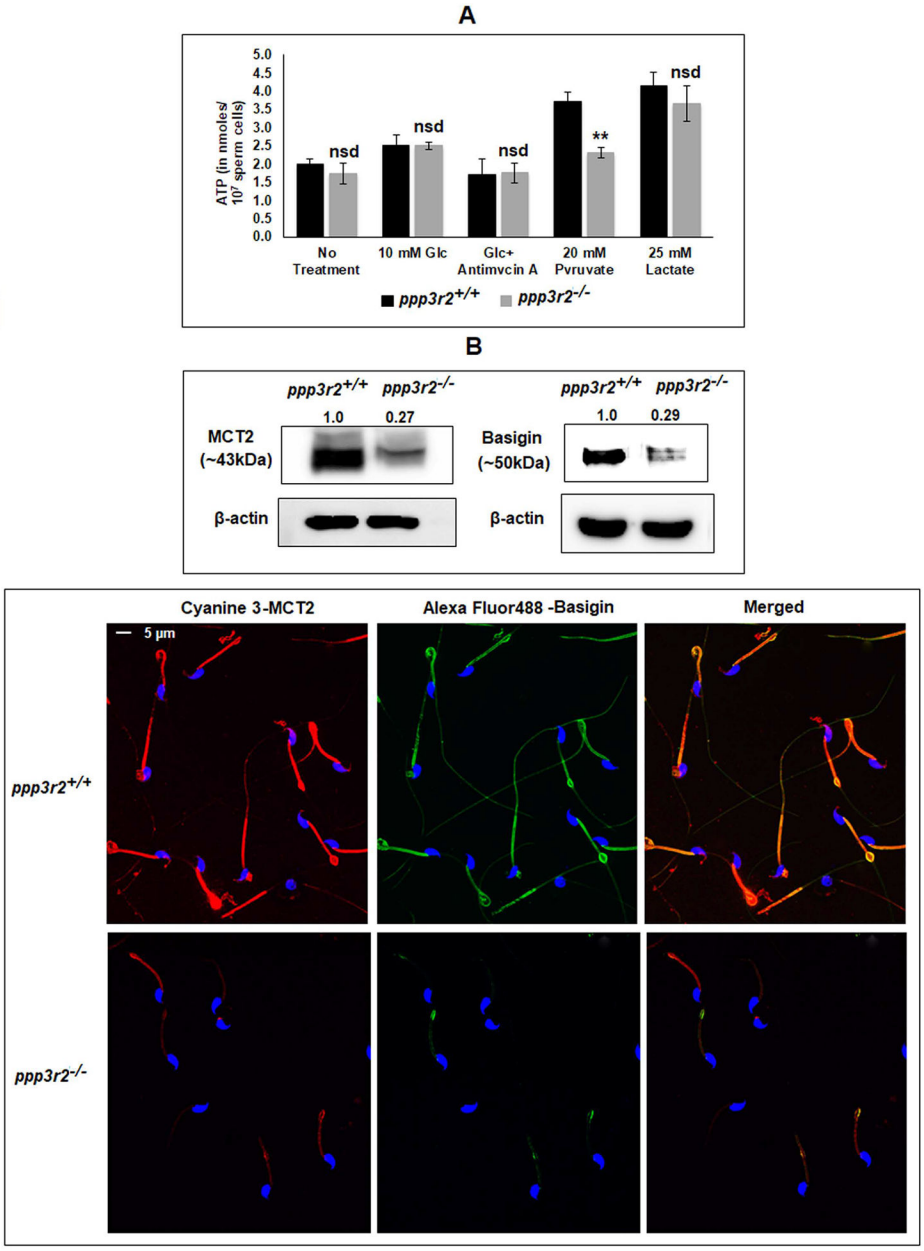

Figure 8: Effect of *ppp3r2* deletion on sperm ATP levels and distribution of monocarboxylate transporter protein complex.

A) Wild type and knock out sperm were incubated in presence or absence of the indicated energy substrates for 1 hour and ATP levels were determined by a luciferase assay as described. ATP level in the *ppp3r2* knockout spermatozoa incubated in presence of pyruvate did not increase as opposed to that of WT sperm population. B) Expression of MCT2 and its binding partner, basigin in calcineurin KO mouse sperm were significantly lower as seen in western blot of whole sperm lysate (upper panel) and immune-cytofluorescence (lower panel) developed by anti-mouse MCT2 and anti-goat EMMPRIN (basigin) antibodies. As loading control for the western blots, mouse monoclonal anti-β-actin antibodies were used; the calculated average band intensities (n=3) provided on top of the corresponding blots. For

immunofluorescence, cyanine 3 and Alexa fluor488 conjugated secondary IgGs were used for MCT2 and basigin, respectively; Hoechst was used for DNA staining. Details of the protocol has been described in materials and methods. Merged picture is in the right-hand corner.

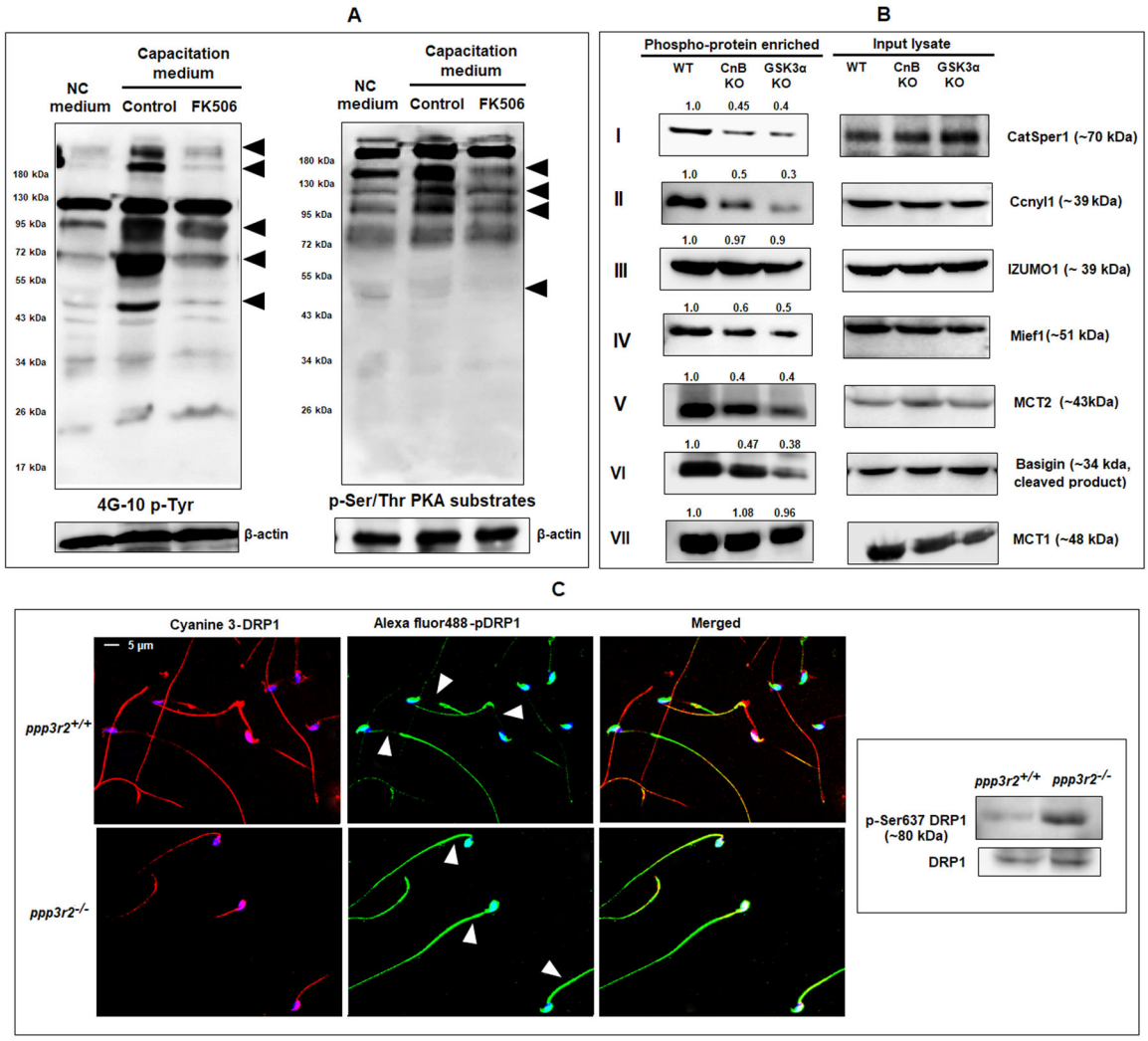

Figure 9: Role of calcineurin in murine sperm protein phosphorylation.

A) During capacitation: Both tyrosine phosphorylated proteins and PKA phosphorylated serine/threonine containing protein profiles were altered under influence of FK506 (20 nM) after 90 min incubation as evidenced by the result of western blot using the anti-mouse 4G10 and anti-rabbit phospho-(ser/thr) PKA substrate antibodies. B), C) Post germ cell differentiation: B) Phosphorylation status of proteins shown were studied by phosphoprotein enrichment analysis. Soluble protein factions extracted from WT, *ppp3r2* (CnB) and GSK3a knockout mouse spermatozoa were subject to phospho-enrichment as described under materials and methods. The phospho-enriched fractions and lysates were subjected to western blot analysis with the indicated antibodies. CatSper1, Ccnyl1, Mief1, MCT2 & basigin showed reduced phosphorylation in both CnB and GSK3α knock sperm, while that of IZUMO1 and MCT1 were unchanged (as indicated by the calculated average band intensities provided on top of the corresponding blots). C) Effect of *ppp3r2* gene deletion on phosphorylation status of mitochondrial fusion marker DRP1 was determined by immune-cytofluorescence (left panel) and western blot of mouse testis extract (right panel).

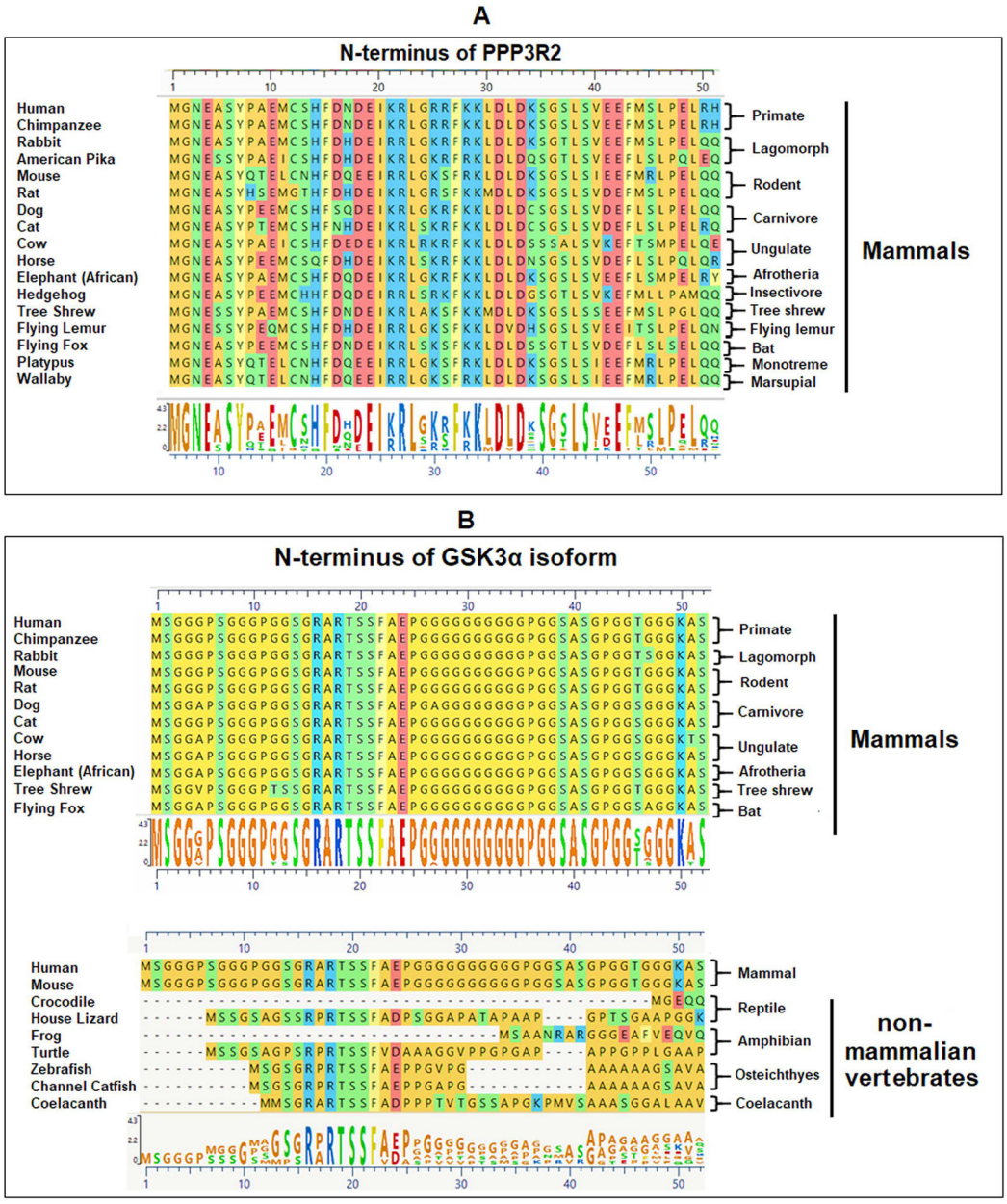

Figure 10: Conservation of PPP3R2 and GSK3α in mammals.

A) PPP3R2 is present in mammals and not in any non-mammalian vertebrate genomes present in ensemble data base. The first 52 amino acids of N-terminus are shown here, which is conserved in mammals including marsupials. B) GSK3α isoform is present in all vertebrates except in avian species. However, the glycine-rich N-terminus of this isoform, is highly conserved in mammals. All the non-mammalian vertebrates show very high degree of variation in their GSK3α amino acid sequences. Sequences were collected from NCBI database and analyzed using Mega Align Pro application of the DNA STAR software; all the sequences were aligned using ClustalW.

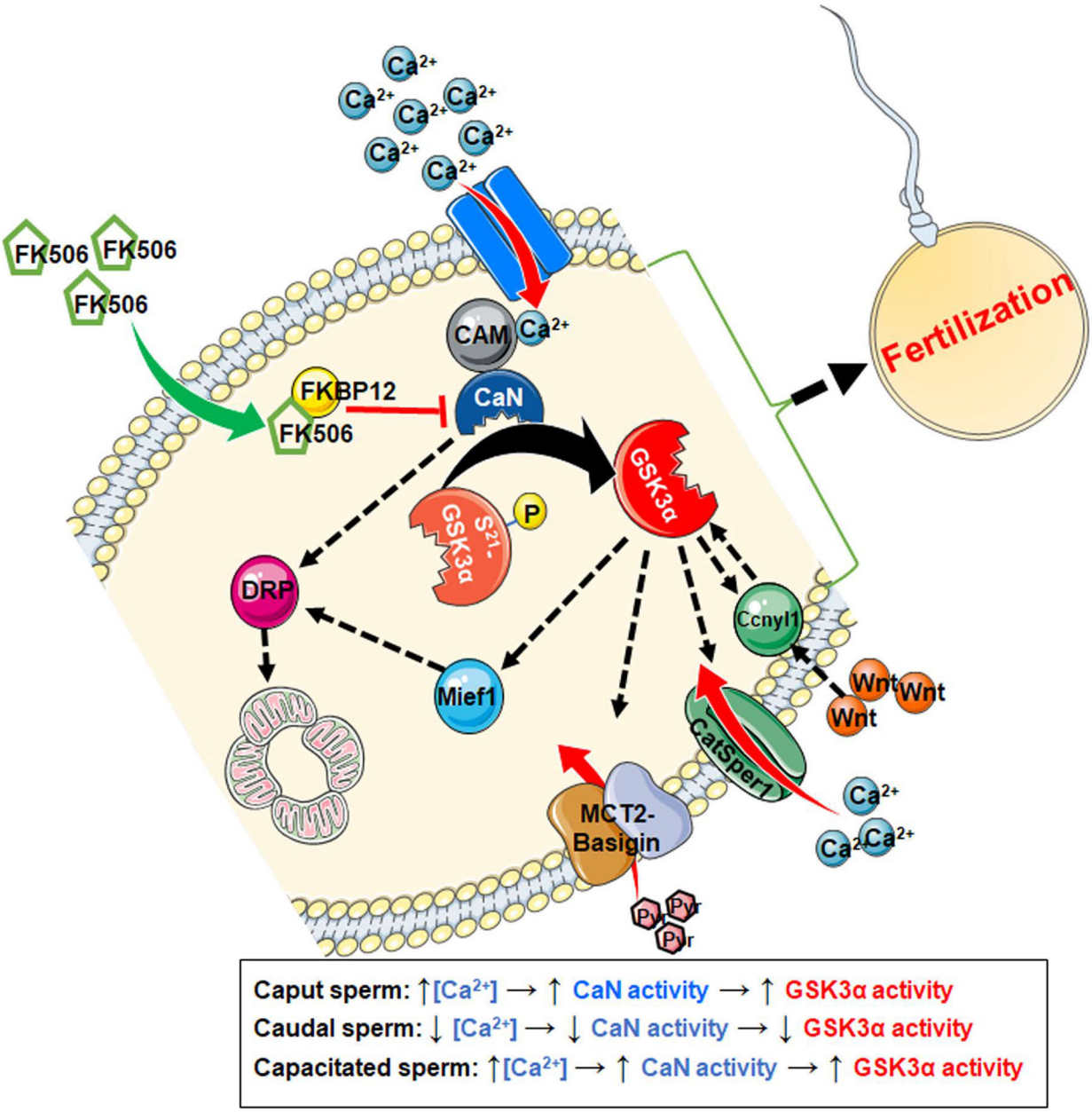

Figure 11: A schematic presentation of the postulated relationship between calcineurin and GSK3α.

Upon activation by the Ca^{2+}-calmodulin complex, calcineurin can dephosphorylate the GSK3α from its inhibitory Ser21 residue. Activation of GSK3α by calcineurin can be prevented by the application of its inhibitor, FK506 at nanomolar concentration. FK506 binds with FKBP12, present inside the sperm and inhibits the catalytic activity of calcineurin. Mief1, MCT2, Basigin, CatSper1 and Ccnyl1 have the S/T(p)-X-X-X-S/T consensus sequence which is normally phosphorylated by GSK3α on the C-terminal S/T of the sequence. DRP1 contains at least two calcineurin binding LxVP sequences.

Table 1:

Intracellular free calcium levels of caudal sperm incubated under capacitating or non-capacitating conditions in the presence or absence of FK506 (20nM) were measured as described in materials and methods. The table also shows calcineurin activity of untreated sperm extracts with the addition of free calcium (found in caput sperm or non-capacitated and capacitated caudal sperm). For comparison, the values for intracellular calcium and calcineurin activity are also shown for caput sperm. Data for calcium levels and calcineurin activity are means ± SEM. *****$[Ca_2^+]_i$ levels shown in the preceding column were used in the corresponding calcineurin activity assay medium; ******20 nM FK506 was added to the calcineurin activity assay medium for this set and it should be treated as the negative control for this activity assay.

Sperm type	Incubating condition	Treatment	Measured $[Ca_2^+]$ (in nM) (n=5)	Corresponding CaN activity (nmol phosphate released/hr) (n=3)*
Caput epididymal sperm	-	-	961±66	1.06±0.084
Caudal epididymal sperm	**Non-capacitating**	-	287±25	0.22±0.02 ($p \leq 0.01$)
	Capacitating	**1% EtOH**	897±52	0.78±0.046
		20 nM FK506	826±55	******0.030±0.004 ($p \leq 0.01$)

Table 2:

Phosphoproteins detected to be differentially phosphorylated in the *Ppp3r2* KO sperm population are either potential targets of GSK3 or calcineurin.

The fourth amino acid (S/T) towards C-terminus (shown in red) from the pre-phosphorylated residue (shown with asterisk) are the potential GSK3 targets.

Phospho-protein	GSK3 phosphorylation consensus sites	Calcnineurin binding motif
	S*/T*xxxS/T	**LxVP; PxIxIT**
MCT2	……S*KVGS*^{214}RHDS^{218}……T*VKAS^{469}……	NA
Basigin	…..S*LNSS^{162}…S*GEYS^{202}…S*EHSS^{233}…T^{283}PEKS^{287}…..	NA
CatSper 1	…T*HPGS^{18}..S*EPLS*^{146}HPSS^{150}….S*TLAT^{260}…S*ILTS^{474}… T*LSGS^{485}..T*TLFT^{429}…	NA
MIEF1	….S*APTS^{59}…S*GCRS^{361}…	NA
CCNYL1	…..T*IFLS^{99}…..S*SCST^{131}…	NA
DRP1	NA	…..L^{412}FVP^{415}…L^{632}DVP^{635}..